

Chapter 2

Sample Controlled Thermal Analysis (SCTA) as a Promising Tool for Kinetic Characterization of Solid-State Reaction and Controlled Material Synthesis

Jose M. Criado, Luis A. Pérez-Maqueda and Nobuyoshi Koga

Abstract The historical development of the thermal analysis methods that imply an intelligent control of the reaction temperature by the own sample (SCTA) is outlined. It has been shown that the precise control of the reaction rate involved in SCTA enables a control, either direct or indirect, of both the partial pressure of the gases generated/consumed by the reaction and the heat evolution/adsorption rate associated to the reaction. This control allows to minimize the influences of heat and mass transfer phenomena and to obtain real kinetic parameters of the forward reaction that occur under the conditions far from the equilibrium. Moreover, it is shown that the shape of α - T plots obtained under constant rate of transformation (CRTA) is strongly dependent on the kinetic model, while the α - T plots obtained using the conventional linear nonisothermal method represent a sigmoidal shape irrespective of the kinetic model. Thus, CRTA has a considerably higher resolution power for discriminating the kinetic model obeyed by the reaction. The applications of SCTA methods both for the kinetic analysis of solid-state reactions and for the synthesis of materials with controlled texture and/or structure have been reviewed. The chapter contains 202 references.

2.1 Introduction to Sample Controlled Thermal Analysis

Sophisticated controls of material synthesis processes are necessary for obtaining the functional materials with desired chemical and physical properties. Among others, thermal treatments involving calcination and annealing processes are of

J.M. Criado (✉) · L.A. Pérez-Maqueda
Instituto de Ciencias de Materiales de Sevilla, Centro Mixto Universidad de Sevilla—C.S.I.C., c/Américo Vespucio 49, 41092 Seville, Spain
e-mail: jmcriado@icmse.csic.es

N. Koga
Chemistry Laboratory, Department of Science Education, Graduate School of Education, Hiroshima University, Higashi-Hiroshima 739-8524, Japan

paramount importance in the synthesis of materials. For developing well-controlled synthesis procedure of the advanced materials via the thermal treatments of precursor materials, the chemical and physical processes that occur in the solid state should be characterized in details. Thermal analysis methods such as thermogravimetry (TG), differential thermal analysis (DTA), differential scanning calorimetry (DSC), and evolved gas analysis (EGA) are extensively used in material characterization including the kinetic analysis of solid-state reactions. In general, all thermal treatments are performed under isothermal or linearly increasing temperature (linear nonisothermal) conditions. Another alternative to perform thermal treatments can be designed by controlling the rate of thermally induced transformation according to predetermined rules, resulting in a smart temperature control where the transformation kinetics of the reaction governs the temperature profile during the course of the process. This technique with the inverse concept of thermal analysis is generally named Sample Controlled Thermal Analysis (SCTA). This alternative approach is realized by monitoring the rate of thermally induced variation of a physical property of the sample that is proportional to the reaction rate. By using a feedback control system, the regulation of variation rate of such property according to predetermined rules determines the temperature profile during the reaction. We will refer along this chapter to one of the SCTA methods, that is, the most generally used technique to control the temperature in such a way that the reaction rate is maintained constant all over the process. The SCTA technique is known as Constant Rate Thermal Analysis (CRTA).

Probably, the first CRTA instrument was that proposed by Smith in 1940s [1]. This method referred to as “Smith Thermal Analysis” [2] used a differential thermocouple to establish a constant temperature difference between sample and furnace wall and is continuously employed even in a modernized form to study alloys systems [3]. The sensitivity of this method has been dramatically improved by Charsley et al. [2], by applying the advantages of CRTA to DSC, named “Sample Controlled Differential Scanning Calorimetry (SCDSC)” [2]. However, the great boost of SCTA methods was driven in the 1960s and 1970s because of the works of two groups, one in France and the other in Hungary. In France, Rouquerol developed that called “Constant Rate Thermal Analysis (CRTA)” [4–6]. This method uses the partial pressure of the evolved gases for monitoring the transformation rate and as feedback signal for controlling sample temperature. Conversely, the Paulik brothers, in Hungary, used the derivative TG (DTG) signal for the same purpose and used the term “quasi-isothermal” for describing the working conditions of their device [7–9]. Different devices for maintaining the reaction rate to be constant during the course of the process have been described in literatures [10–13]. Since then, other approaches have been proposed in literatures, it is worth citing that of Sørensen, called “Stepwise Isothermal Analysis” [14]. In this method, the sample temperature is increased at a constant heating rate until the reaction rate reaches a pre-set limit, then the temperature remains constant until the reaction rate reaches a lower pre-set limit, when the heating is reassumed. Parkes et al. [15] proposed another approach, in which the sample temperature is maintained at a constant, while the partial pressure of the reactive gas is adjusted so as to keep the

reaction rate to be constant. Other authors have proposed a new form where the reaction rate is steadily accelerated, providing better resolution for kinetic analysis [16, 17]. Recently, most of commercially available thermal analysis devices are equipped with the SCTA methodologies in their most modern instruments, while proposing new modified approaches such as high-resolution thermal analysis (High-ResTM) introduced by TA Instruments[®] [18] or Max-ResTM included in the software of Mettler[®].

The developments of SCTA techniques are expected to expand the application of the quantitative analysis for the changes in the physico-chemical properties of materials during thermally induced transformation process to the complex process by realizing the higher experimental resolution for deconvoluting partially overlapping multistep reaction. An illustrative example is the application of SCTA to the compositional analysis of multicomponent polymeric materials. Figure 2.1 compares the mass-change curves recorded in flowing N₂ under the conventional linear heating condition at a heating rate β of 1 K min⁻¹ and under CRTA control at a C ($= dz/dt$) of 3.0×10^{-3} min⁻¹ for PVC blended with a plasticizer, DINCH (1, 2cyclohexane dicarboxylic acid, diisononyl ester) [19]. The temperature profile of CRTA apparently indicates well separated two-step mass-change process composed of the evaporation of the plasticizer and the thermal degradation of the polymer, while the two-step process cannot be distinguished in the conventional TG. Thus, SCTA can be used to determining the percentage of plasticizers contained in blended polymers, as well as chromatographic techniques [20, 21].

SCTA is also promising for solving long-discussed methodological problems inherent in the kinetic analysis of solid-state reaction using thermal analysis and for precisely controlling the morphology and structure of solid products in the material synthesis via the thermal treatment of solid precursors. In this chapter, the merits of SCTA for applying to the kinetic analysis of solid-state reactions and to the morphological and structural controls of solid products during the solid-state reactions are described as exemplified by some practical examples.

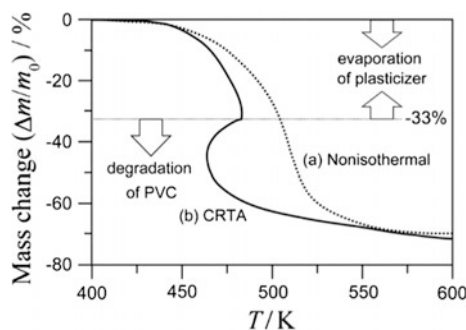


Fig. 2.1 Comparison of mass-change traces of a blended PVC–DINCH recorded in flowing N₂: **a** under linear heating condition at β of 1 K min⁻¹ and **b** under constant transformation rate condition at C ($= dz/dt$) of 3.0×10^{-3} min⁻¹ [19, 22]

2.2 Advantages of SCTA for Recording Kinetic Rate Data

The kinetic analysis of the solid-state reactions is a scientific methodology constructed with different components involving the measurement of kinetic rate data, kinetic theory, and kinetic calculation [23]. As the measurement technique, various thermal analysis methods have widely been used for tracking of the reaction processes of solid-state reactions. The simplified kinetic equation with the assumption of the single step reaction regulated by a specific rate-limiting step is used in many kinetic studies [24, 25].

$$\frac{d\alpha}{dt} = A \exp\left(-\frac{E_a}{RT}\right) f(\alpha) \quad (2.1)$$

where α is the reacted fraction at time t ; E_a is the apparent activation energy; A is the pre-exponential factor of Arrhenius; T is the absolute temperature; and $f(\alpha)$ is a function depending on the physico-geometrical mechanism of the reaction [26]. Many different calculation methods have been proposed for determining the kinetic parameters, i.e. E_a , A , $f(\alpha)$, and kinetic exponents in $f(\alpha)$, by applying Eq. (2.1) to the analysis of experimentally resolved thermoanalytical curves [27, 28]. The experimentally determined kinetic parameters are used for discussing the kinetic characteristics of the reaction, for evaluating possible change in the kinetics depending on reaction conditions, and for comparing the kinetic characteristics among a series of samples and reactions. In this scheme, any drawbacks in each methodological component possibly affect the physical significance of the apparent kinetic parameters. Therefore, further developments of each methodological component are necessary for promoting the methodology to be more powerful tool for researches in modern material sciences [23, 25]. At the same time, each methodological component should compensate the drawbacks in the others for establishing the logically coordinated methodology for kinetic analysis that is fully supported by chemistry and physics.

The measurement of kinetic rate data is essential for the reliable kinetic analysis. The precise measurements realized using modern thermoanalytical instruments do not necessarily provide the reliable kinetic rate data. This relates to the other methodological components, that is, the kinetic theory illustrated by the fundamental kinetic equation and the kinetic calculation method employed for the data analysis. In the fundamental kinetic equation Eq. (2.1), the reaction rate is expressed only as the functions of T and α , and no other factors that affect the reaction rate is assumed. This simplified assumption is rarely realized in the actual solid-state reactions, because of the heat evolution/absorption and generation/consumption of gases during the reaction. The apparent reaction rate is more or less influenced by the self-generated reaction conditions and those changes during the reaction, which is not considered in the fundamental kinetic equation. Therefore, careful considerations of the sample and measurement conditions are

requested for minimizing the influences of mass and heat transfer phenomena on the apparent reaction rate behaviour [29]. SCTA have important advantages for tracking of the kinetic rate data of solid-state reactions with regard to the conventional linear nonisothermal and even isothermal methods. The precise control of the reaction rate involved in SCTA enables a control, either direct or indirect, of both the partial pressure of the gases generated/consumed by the reaction and the associated heat evolution/adsorption rate during the course. This control allows to minimize the influences of heat and mass transfer phenomena and to obtain real kinetic parameters of the forward reaction that occur under the conditions far from the equilibrium.

Figure 2.2 compares the TG–DTG curves for the thermal decomposition of NaHCO_3 under isothermal, linear nonisothermal, and CRTA conditions [30] drawn as a function of time, which is in accordance with that illustrated conceptually by Reading [31, 32] and clearly describes the differences of the experimentally resolved thermoanalytical data as a source of kinetic rate data in view of the control of self-generated reaction conditions during the reaction. The shape of the DTG curves is directly correlated to the variations in the rates of gaseous evolution and heat exchange during the reaction. It is thus apparent that the variations in the rates of gaseous evolution and heat exchange are the most significant for the thermoanalytical data recorded under linear nonisothermal conditions, although the magnitudes change depending on the applied measurement conditions involving sample mass, heating rate, flow rate of inert gas, and so on. The variations are largely

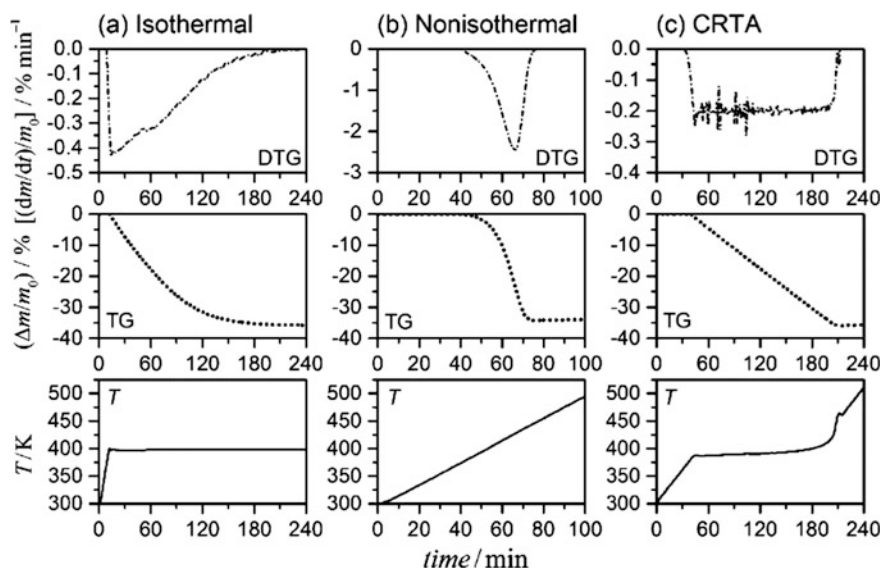


Fig. 2.2 TG–DTG curves for the thermal decomposition of NaHCO_3 (100–170 mesh, sample mass $m_0 = 5.0$ mg, in flowing N_2 ($80 \text{ cm}^3 \text{ min}^{-1}$)) recorded under **a** isothermal ($T = 398$ K), **b** linear nonisothermal ($\beta = 2 \text{ K min}^{-1}$), and **c** CRTA ($C = 10.0 \text{ } \mu\text{g min}^{-1}$) conditions [30]

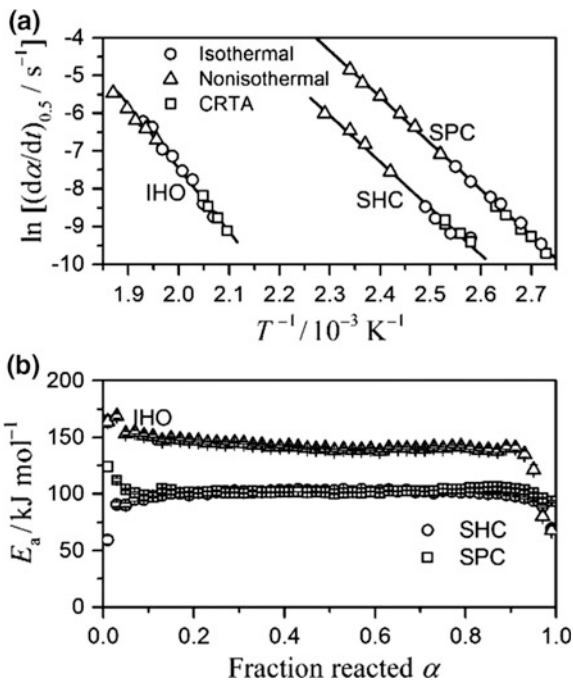
diminished in the isothermal measurements, but still cannot be ignored. If the variation rate of a physical property for a single step reaction, mass-change rate in the example of Fig. 2.2, was controlled to be constant as in CRTA, no variations of the rates of gaseous evolution and heat exchange are practically found. The differences among the thermoanalytical data recorded under different temperature control modes produce different self-generated reaction conditions during the reaction and possibly cause the different influences of the mass and heat transfer phenomena on the apparent kinetic behaviour. Even under such different reaction conditions produced by the reaction, all of the kinetic rate data recorded under different temperature control modes are equally useful for the kinetic analysis based on Eq. (2.1), if the reaction rate of a single step reaction was not sensitive to the variations in the partial pressure of the evolved gas, and the appropriate measurement conditions were selected for realizing negligible temperature gradient within the sample. The establishment of the ideal situation is confirmed by examining the isoconversional relationship (Eq. 2.2) among the data points at a fixed α extracted from a series of kinetic rate data recorded under different temperature control modes and the constancy of the evaluated E_a values at different α during the course of reaction, because Eq. (2.1) is applicable to all of the kinetic rate data under different temperature controlled modes [33, 34].

$$\ln\left(\frac{d\alpha}{dt}\right)_\alpha = \ln[Af(\alpha)] - \frac{E_a}{RT_\alpha} \quad (2.2)$$

Such ideal kinetic behaviour in view of simplicity of the kinetic analysis is actually observed in the practical reactions as is illustrated in Fig. 2.3 for the kinetic analysis of the thermal decompositions of NaHCO_3 [30], $\text{In}(\text{OH})_3$ [35], and $\text{Na}_2\text{CO}_3 \cdot (3/2)\text{H}_2\text{O}$ [36]. In these examples, the isoconversional plot of $\ln(d\alpha/dt)$ versus T^{-1} , known as the Friedman plot [37], for the data points at the fixed α are appreciably linear and the E_a values are practically constant in a wide range of α . In the isoconversional kinetic relationship, the data points obtained from the measurements using CRTA take over the lower reaction rate and temperature part in the kinetic relationship. In general, the lower the reaction rate is the higher the chance to diminish the gradients of temperature and partial pressure of evolved gas in the sample matrix. Therefore, the data points of CRTA can be used as the reference for examining the applicability of the thermoanalytical data recorded using the conventional isothermal and linear nonisothermal methods and appropriate range of the temperature program parameters, T and β .

The advantage of CRTA in terms of maintaining constant the partial pressure of product gas and the reaction rate at a possibly small constant value is of paramount importance in the case of the kinetic analysis of reversible reactions in the thermal decomposition of solids; $\text{A(s)} \rightleftharpoons \text{B(s)} + \text{C(g)}$. In such a case, the reaction rate should be expressed by considering the partial pressure, P , of the gaseous product and the equilibrium pressure, P_{eq} , of the reaction [24, 38]:

Fig. 2.3 Isoconversional kinetic analyses for the thermal decompositions of NaHCO_3 (SHC) [30], $\text{in}(\text{OH})_3$ (IHO) [35], and $\text{Na}_2\text{CO}_3 \cdot (3/2) \text{H}_2\text{O}_2$ (SPC) [36]: **a** Friedman plots at $\alpha = 0.5$ and **b** E_a values at different α



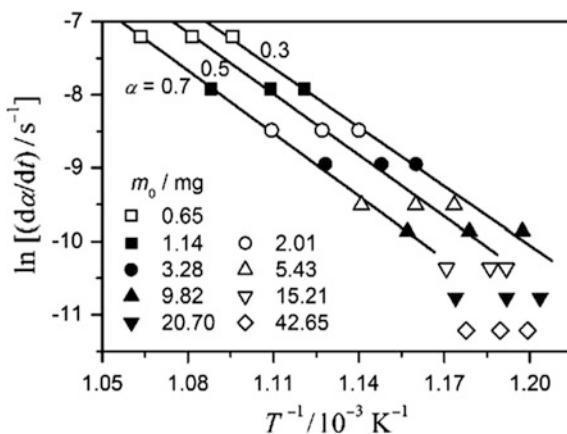
$$\frac{d\alpha}{dt} = A \exp\left(-\frac{E_a}{RT}\right) f(\alpha) \left(1 - \frac{P}{P_{\text{eq}}}\right) \quad \text{with } P_{\text{eq}} = \exp\left(\frac{\Delta_r S}{R}\right) \exp\left(-\frac{\Delta_r H}{RT}\right) \quad (2.3)$$

where $\Delta_r S$ and $\Delta_r H$ are the entropy and the enthalpy of the reaction, respectively. It is clear from Eq. (2.3) that the term $(1 - P/P_{\text{eq}})$ should be maintained close to unity in order to obtain reliable kinetic parameters for the forward reaction represented by Eq. (2.1). If the value of P were strictly controlled or precisely measured through the overall reaction, it would be possible to carry out a meaningful kinetic analysis using Eq. (2.3), for which SCTA is a proper method. On the other hand, the isothermal and linear nonisothermal temperature control methods (Fig. 2.2) would lead to significant changes in the reaction rate and in the partial pressure of the product gas, which generally cannot be controlled and could modify the shape of the thermoanalytical curves leading to a meaningless interpretation of the reaction mechanism. Owing to the good control of both the atmosphere surrounding the sample and the real temperature of the sample bed exerted by SCTA methods, the E_a values determined for either reversible [39–52] or irreversible [53] thermal decompositions of solids were sometimes independent of the starting sample mass m_0 in a wider range, while a similar behaviour was not observed when the measurements under linear nonisothermal conditions were concerned. For example, Criado et al. [39] reported that the E_a value for the thermal decomposition of CaCO_3 ; $\text{CaCO}_3 \rightleftharpoons \text{CaO} + \text{CO}_2$, as determined under a high dynamic vacuum

using SCTA experiments, was independent of m_0 in the investigated range, i.e. from 0.5 to 50 mg. However, the E_a value determined from conventional linear heating TG curves under high vacuum is strongly depending on the experimental conditions. For obtaining the relevant E_a value with reference to that determined using SCTA, the measurement conditions using m_0 less than 2 mg and β lower than 1 K min^{-1} were necessary in the linear nonisothermal measurement. These results are consistent with those reported later by Reading et al. [42] for the same reaction. Koga and Criado [51] investigated more critically the range of m_0 where the influence of the mass transfer phenomena is practically negligible during CRTA measurements for the thermal decomposition of CaCO_3 under high vacuum, in which a series of CRTA curves under high vacuum was recorded by controlling the evolution rate of CO_2 to be a fixed constant value and by changing m_0 . As shown in Fig. 2.4, the effect of the mass transfer phenomena on the apparent kinetic behaviour appears to be practically negligible in a smaller m_0 range ($m_0 < 10 \text{ mg}$), where the isoconversional relationship was actually established. This ideal situation was suddenly broken due to the influence of the mass transfer phenomena when m_0 was attained a certain value, although the critical m_0 value is the empirical value that varies with the size of sample pan, sampling conditions, and controlled vacuum.

In the case of the thermal decomposition of CdCO_3 and PbCO_3 , it was further difficult to obtain E_a values independent of m_0 and β from conventional linear nonisothermal measurements, while the E_a values obtained from SCTA were practically constant in a wide range of m_0 [41]. The similar conclusion was derived by Ortega et al. [44, 49] through the kinetic study of the thermal decomposition of dolomite. From those results, SCTA can be recognized as one of the most reliable approaches for obtaining meaningful kinetic parameters for the thermal decomposition of solids. The influence of the partial pressure of the product gas around the sample on the kinetic results analyzed by several authors [46, 55, 56] indicated that, in the case of reversible reaction, a poor control of the pressure would lead to

Fig. 2.4 Friedman plots at different α for the thermal decomposition of CaCO_3 under high vacuum ($5.0 \times 10^{-3} \text{ Pa}$) examined for a series of CRTA curves recorded by controlling the transformation rate to be a fixed constant value and by changing m_0 [51, 54]. (Reproduced from [54] with permission)



artificially high E_a values as is expected from Fig. 2.4, although reliable kinetic parameters of the forward reaction could be obtained by introducing an accommodation function for the partial pressure of product gas [56] in the general kinetic equation as in Eq. (2.3), if the partial pressure of the product gas around the sample is known or measured.

Rouquerol et al. [57, 58] proved that even a relatively small change of the partial pressure of the product gas in the high vacuum range could influence on the reaction mechanism of the thermal dehydration of inorganic hydrates. This behaviour would explain that the E_a values obtained from SCTA methods are independent of m_0 in an appreciably wide range, while the kinetic parameters obtained from conventional linear nonisothermal method very often depend on m_0 and β . This is because all the kinetic analyses of reversible reactions referred in the previous paragraph had been carried out using experimental SCTA data recorded under vacuum and at a low constant partial pressure of the product gas during the course of reaction. The ideal reaction conditions were realized by employing instruments based on the method originally developed by Rouquerol [4–6], where the sample temperature was regulated so as to control the residual pressure to be a low constant value. As the results, the influence of the mass transfer phenomena on the experimentally resolved thermoanalytical curve is minimized and the accommodation function for the partial pressure of the product gas in Eq. (2.3), $(1 - P/P_{eq})$, can be treated approximately as unity or a constant. It has been shown by Criado et al. [39] that it is difficult to maintain the partial pressure of CO_2 during the thermal decomposition of CaCO_3 to be a constant in the conventional linear nonisothermal measurement, even if a dynamic starting vacuum of 2.6×10^{-4} Pa was applied using a high pumping rate vacuum system. For example, when the TG curve for the thermal decomposition of CaCO_3 with m_0 of 21 mg was measured at a β of 10 K min^{-1} in the dynamic vacuum system, the partial pressure of CO_2 increased up to approximately 10^{-1} Pa. To keep the starting pressure of 2.6×10^{-4} Pa during the thermal decomposition, m_0 and β should be decreased to 1 mg and 0.5 K min^{-1} , respectively. However, mass-loss curves at a constant pressure as low as 5×10^{-4} Pa during entire course of the thermal decomposition were recorded, under SCTA conditions, irrespective of m_0 . Furthermore, the thermal decomposition of BaCO_3 was studied using SCTA under constant residual partial pressures of CO_2 lower than 10^{-5} Pa by using a high vacuum system equipped with a mass spectrometer attached to a thermobalance [59]. In this case, the partial pressure of CO_2 evolved by the reaction was directly monitored during the entire experiment by means of the mass spectrometer, and even partial pressures lower than the total limit vacuum of the system are used for the feedback control of the sample temperature. Using this procedure, the thermal decompositions of very stable compounds with low equilibrium pressures could be studied in conditions far from equilibrium. Further complex cases can be found for the thermal decomposition of solids that evolves more than one gas and each evolved gas influences differently on the apparent kinetic behaviour. Koga et al. [13, 54, 60–63] approached to the complex kinetic behaviour observed for the thermal decompositions of NaHCO_3 , $\text{Cu}_2\text{CO}_3(\text{OH})_2$ (synthetic malachite), and $\text{Zn}_5(\text{CO}_3)_2(\text{OH})_6$ (synthetic hydrozincite),

using an instrument of constant rate EGA (CREGA) coupled with TG, in which the concentrations of CO_2 and H_2O in the inlet gas to TG were systematically varied and the changes in CO_2 and H_2O concentrations in the outlet gas from TG were controlled to be constant values using CRTA technique. Through examining the thermal decomposition processes that simultaneously evolve CO_2 and H_2O under systematically varied conditions of applied and controlled concentrations of CO_2 and H_2O , it was revealed for the thermal decompositions that CO_2 indicates normal effect on the apparent kinetic behaviour in view of chemical equilibrium, while H_2O exhibits the inverse effect.

The possible thermal gradient within the sample matrix induced by self-cooling or self-heating by the enthalpy of the reaction and the influences of heat transfer phenomena on the experimentally resolved shape of thermoanalytical curves can also be diminished by the application of SCTA. This advantage is used for studying significant exothermic reactions that lead ignition of the sample under conventional thermal analysis method. In SCTA, the self-heating effect by the exothermic reaction can be regulated by controlling the transformation rate during the entire course of the reaction; therefore, preventing thermal runaway and ignition as was demonstrated by Charsley et al. [2] in the study of metal-oxidant pyrotechnics. Paulik [64] has reviewed the successful applications of SCTA for the study of exothermic reactions.

Despite of the problems concerning mass and heat transfer phenomena, application of periodical rate jump during the CRTA measurement proposed by Rouquerol [65–67] can be used for determining reliable E_a value even using a larger m_0 . The CRTA jump method imposes periodical jumps between two pre-set reaction rates, C_1 and C_2 , and records the accompanied change in the sample temperature from T_1 to T_2 . Because the transformation rate is originally controlled at a low constant rate in CRTA, the fraction reacted at times just before and after the rate jump can be approximated to a constant value. Then, using the two data sets of controlled rate and temperature, (C_1, T_1) and (C_2, T_2) , the E_a value can be calculated in an isoconversional scheme.

$$E_a = \frac{RT_1T_2}{T_2 - T_1} \ln \frac{C_2}{C_1} \quad (2.4)$$

As in the Friedman plot based on Eq. (2.2), the kinetic model function is cancelled between the two states. It was reported in many kinetic studies of the thermal decomposition of solids, the E_a values at different rate jump points are practically constant and reasonable in comparison with other data sources [44, 68], indicating the practical usability to determine the E_a value from a single CRTA rate jump measurement.

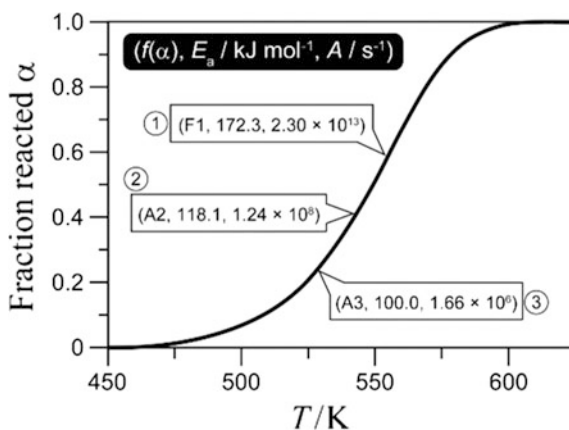
The above review results support our primary statement concerning the advantage of SCTA and allow us to conclude that SCTA methods are a more reliable approach than conventional linear nonisothermal methods in order to obtain reliable E_a values for the thermal decomposition of solids.

2.3 Merits of Kinetic Calculation Using CRTA Curves

The resolution power of SCTA for discriminating among the reaction kinetic models of solid-state reactions listed in Ref. [24] is somewhat more favourable than that of isothermal methods and considerably higher than that of conventional linear nonisothermal methods. This analysis will be mainly based on CRTA that has been the most extensively and systematically studied among different SCTA methods in literatures, as shown in previous reviews on the topic [31, 32, 69]. The characteristic of CRTA is especially important when a single thermoanalytical curve is subjected to the kinetic analysis. However, various kinetic calculation methods using a single thermoanalytical curve recorded under linearly increasing temperature have been proposed and widely used because of less laborious procedure. However, the single run methods have an apparent drawback of mutually correlated apparent variations of calculated kinetic parameters involving E_a , A , and $f(\alpha)$ [70]. This problem is clearly illustrated by curve fittings of a single α - T plot under linear nonisothermal condition using different kinetic models as shown in Fig. 2.5 [71, 72]. By assuming F1, A2, and A3 models, the uniform α - T plot can be reproduced within an error lower than $10^{-5}\%$, where different sets of Arrhenius parameters, E_a and A , are estimated for the respective $f(\alpha)$ assumed. Therefore, the mutual correlation of the calculated kinetic parameters leads the distortion of the calculated E_a and A values due to the wrong choice of $f(\alpha)$ and a superficial linear correlation between E_a and $\ln A$ values calculated by assuming different kinetic model functions [70, 73–77]. The distortion of the Arrhenius parameters by the wrong choice of the kinetic model function can be explained as a simple mathematical relationship using an approximation of exponential temperature integral under linearly increasing temperature condition [78, 79].

$$\frac{E_{\text{dis}}}{E_a} = \frac{f(\alpha_p)F'(\alpha_p)}{F(\alpha_p)f'(\alpha_p)} \quad \text{with } f'(\alpha) = \frac{df(\alpha)}{d\alpha} \quad \text{and } F'(\alpha) = \frac{dF(\alpha)}{d\alpha} \quad (2.5)$$

Fig. 2.5 A single TG curve at β of 1 K min^{-1} drawn by assuming three different kinetic models with different Arrhenius parameters ($f(\alpha)$, $E_a/\text{kJ mol}^{-1}$, A/s^{-1}) = (F1, 172.3, 2.30×10^{13}), (A2, 118.1, 1.24×10^8), and (A3, 100.0, 1.66×10^6) [71, 72, 84]



$$\ln\left(\frac{A_{\text{dis}}}{A}\right) = \frac{E_a}{RT_p} \left[\frac{f(\alpha_p)F'(\alpha_p) - F(\alpha_p)f'(\alpha_p)}{F(\alpha_p)f'(\alpha_p)} \right] + \ln \frac{f(\alpha_p)}{F(\alpha_p)} \quad (2.6)$$

where E_{dis} and A_{dis} are the distorted Arrhenius parameters caused by the use of wrong kinetic model function $F(\alpha)$. The subscript p denotes the values at the peak top of the transformation rate under linearly increasing temperature condition. To avoid this problem, it is generally recommended to use a two-step kinetic calculation procedure using a series of thermoanalytical data recorded under different measurement conditions, which is composed of the determination of E_a value as the first step using the isoconversional method and subsequent determination of A and $f(\alpha)$ using the master plot method [28, 34, 80–82]. The single step kinetic calculation based on Eq. (2.1) using multiple thermoanalytical data proposed by Pérez-Maqueda et al. [83] as the combined kinetic analysis method is also useful to avoid the problem. In connection with this problem, the higher power of CRTA for discriminating the kinetic model function provides the possible opportunity of the determination or estimation of the kinetic model function in the first step using a single CRTA curve.

Because in CRTA, the transformation rate is kept constant at a programmed value C , Eq. (2.1) can be rewritten in the following form

$$C = A \exp\left(-\frac{E_a}{RT}\right) f(\alpha) \quad (2.7)$$

In the scheme of constant transformation rate, the shape of CRTA curves characterized by T – α plots (inverse to α – T plots of linear nonisothermal measurements because of inverse measurement logics) are strongly depending on the typical kinetic model functions for the solid-state reactions [71, 85], while the α – T plots obtained using the conventional linear nonisothermal method at a β represent a sigmoidal shape irrespective of the kinetic model. Thus, it is quite impossible to discern the reaction mechanism from the shape analysis of a single TG curve recorded under linear nonisothermal condition [86–93]. The shape analysis of T – α plots of CRTA curves with respect to different $f(\alpha)$ would be very illustrative for demonstrating the power of CRTA for discriminating the most appropriate $f(\alpha)$ from a single experimental curve. Figure 2.6 compares the shapes of T – α plots of CRTA curves drawn by assuming different $f(\alpha)$ functions [54, 72, 94]. It is clearly seen that the T – α plots for the phase boundary controlled models (Rn) are concave with regards to α axis, while those of diffusion controlled models (Dn) present an inflection point. From the difference in the shape of T – α plots, the reactions that obey to Rn and Dn models are distinguishable. However, this observation is applicable to the reaction of the uniformly sized reactant particles, because the shape of CRTA curves for the reaction of interface shrinkage type including Rn and Dn changes depending on the degree of distribution in the particle size [95, 96].

The T – α plots for the Avrami–Erofeev (Am) equation that describes a nucleation-growth model show a minimum temperature midway through the

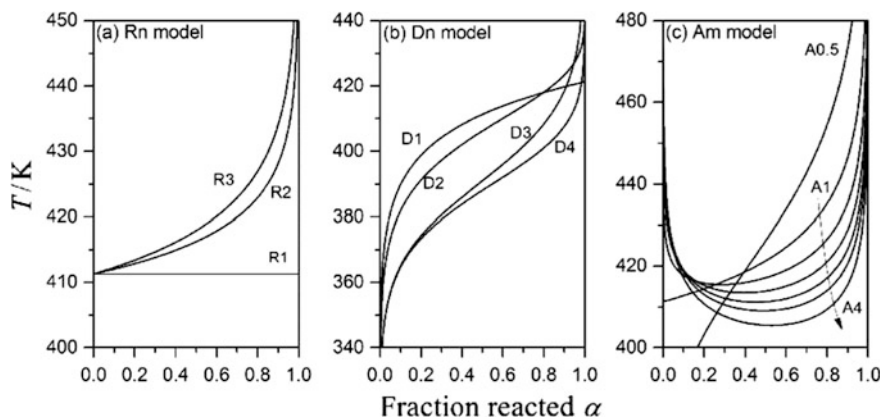


Fig. 2.6 T - α profiles of CRTA curves corresponding to different kinetic models simulated assuming $E_a = 100 \text{ kJ mol}^{-1}$, $A = 5.0 \times 10^8 \text{ s}^{-1}$, and $C (= dz/dt) = 1.0 \times 10^{-4} \text{ s}^{-1}$ [54, 72, 94]. (Reproduced from [54] with permission)

reaction when $m > 1$. By this characteristic of the shape of CRTA curve, the reaction of Am models can be distinguished from Rn and Dn models. The α value at the minimum temperature (α_m) has the specific values for respective Am equations with different kinetic exponents ($\alpha_m = 0.393$; 0.486 ; and 0.528 for the models A2, A3 and A4, respectively) [71]. The α_m values calculated for CRTA curves for Am model are perfectly in agreement with the calculated α value at the maximum transformation rate under isothermal conditions [38, 97]. The relationship between the rate behaviour under isothermal condition and the T - α profile of CRTA for Am models was clearly described by Tiernan et al. [98]. The initial temperature decreasing part in the T - α profile of CRTA would correspond to the acceleratory period under isothermal condition, where the total area of the reaction interface increases by the nucleation and growth of the nuclei. In CRTA, the acceleration would be offset by a diminution of the temperature in order to maintain the transformation rate constant. The later rising temperature stage of CRTA would correspond to the decay period under isothermal condition, where the reaction rate decelerated by the overlapping of the growing nuclei. The deceleration must be compensated by increasing the temperature in CRTA. The specific value of α_m for each Am model can be used for discriminating the most appropriate kinetic exponent among different Am models. A similar T - α profile with the minimum temperature midway through the reaction would be observed for the reaction that indicates a sigmoidal mass-change trace under isothermal condition. The typical examples are the consecutive surface reaction and subsequent shrinkage of the reaction interface towards the centre of the reacting particle as have been formalized under isothermal condition by Mampel [99], autocatalytic reaction formalized by Prout and Tompkins [100, 101], and random scission mechanism of the thermally induced polymer degradation [102, 103]. For effectively using the model discrimination power of CRTA, different master plot methods applicable to shape analysis of CRTA curves have been proposed as reviewed previously [72].

Many practical examples substantiate the higher model discrimination power of CRTA. For example, the thermal decomposition of anhydrous nickel nitrate obeys Am model with $m = 2$ under isothermal conditions [104]. As shown in Fig. 2.7a, the T - α profile of CRTA for the reaction apparently indicates the minimum temperature midway through the reaction at $\alpha_m = 0.38$ [71], which closely corresponds to the specific α_m value for A2 model ($\alpha_m = 0.393$). The T - α profiles of CRTA that are characteristic for Am models have been very often reported in literature for different reactions [57, 58, 62, 64, 105–113], which involves the thermal dehydration of uranyl nitrate trihydrate reported by Bordère et al. [58] as shown in Fig. 2.7b.

Barnes et al. reported an example that effectively utilized the deconvolution power of partially overlapping reaction processes and the discrimination power of kinetic models of SCTA for the thermally induced successive reduction of V_2O_5 to V_2O_3 in hydrogen atmosphere [106, 114]. The reaction steps involved cannot be separated in the conventional linear nonisothermal measurement, while possible three reaction steps, $V_2O_5 \rightarrow V_4O_9 \rightarrow VO_2 \rightarrow V_2O_3$, are expected from the overall α - T profile of CRTA as shown in Fig. 2.8. At the same time, Am models are estimated for the respective reaction steps, because the α - T profiles of all the

Fig. 2.7 T - α profiles of CRTA for **a** the thermal decomposition of anhydrous nickel nitrate under vacuum at $C (= d\alpha/dt) = 4.17 \times 10^{-5} \text{ s}^{-1}$ [71] and **b** thermal dehydration of uranyl nitrate trihydrate under vacuum at $C (= d\alpha/dt) = 2.77 \times 10^{-6} \text{ s}^{-1}$ [58]

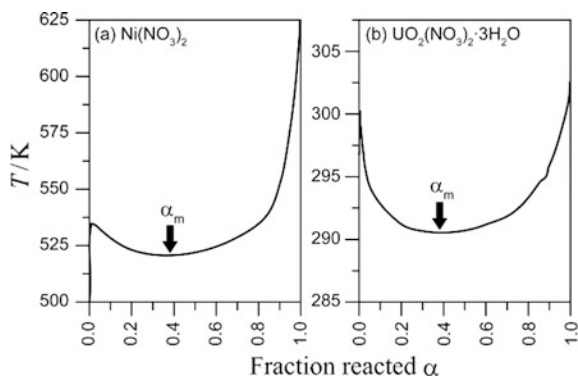
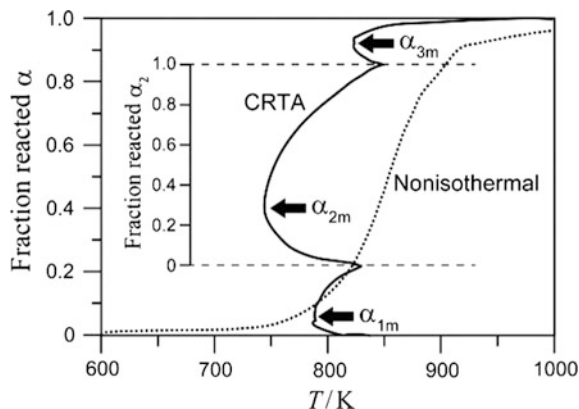


Fig. 2.8 α - T profiles of thermally induced hydrogen reduction of V_2O_5 under linear nonisothermal condition at $\beta = 1 \text{ K min}^{-1}$ and under CRTA condition at $C (= d\alpha/dt) = 1.8 \times 10^{-5} \text{ s}^{-1}$ [106, 114]



reaction steps indicate the characteristic shape for Am model with the minimum temperature midway through the reaction. Tierman et al. [98] have reported the similar effective use of CRTA in their comparative study for the thermal reduction of different iron oxides involving hematite and magnetite. The thermal reduction of hematite to metal iron under conventional conditions are recorded as two overlapping processes, while in CRTA, the two reaction steps are observed separately as a complete conversion to magnetite before the reduction of magnetite to iron takes place. It was also revealed that the reductions of hematite to magnetite and of magnetite to metal iron follow an Rn model and an Am model, respectively. Similarly, the thermal reductions of NiO and CuO have also been studied using CRTA by the same authors, concluding that the shape of the curves is characteristic of an Am model [98, 115].

In some kinetic studies of the thermal decomposition of inorganic solids reported recently, the characteristic $T-\alpha$ profile in CRTA curves with the minimum temperature midway through the reaction were interpreted in relation to physico-geometrical reaction mechanisms other than Am models. For the thermal decomposition of $\text{FeC}_2\text{O}_4 \cdot 2\text{H}_2\text{O}$ [116], the $T-\alpha$ profile of CRTA was explained by the consecutive process of surface reaction regulated by the first order law (F1) and subsequent phase boundary reaction with two dimensional shrinkage of the reaction interface (R2), which is expressed by a kinetic equation of Mampel type under isothermal conditions.

$$(a) \quad t \leq 1/k_{\text{PBR}}$$

$$\frac{d\alpha}{dt} = -2k_{\text{PBR}} \left[\left(1 + \frac{k_{\text{PBR}}}{k_{\text{SR}}} \right) \exp(-k_{\text{SR}}t) + k_{\text{PBR}}t - \left(1 + \frac{k_{\text{PBR}}}{k_{\text{SR}}} \right) \right] \quad (2.8)$$

$$(b) \quad t \geq 1/k_{\text{PBR}}$$

$$\frac{d\alpha}{dt} = -2k_{\text{PBR}} \exp(-k_{\text{SR}}t) \left[1 + \frac{k_{\text{PBR}}}{k_{\text{SR}}} - \frac{k_{\text{PBR}}}{k_{\text{SR}}} \exp\left(\frac{k_{\text{SR}}}{k_{\text{PBR}}}\right) \right] \quad (2.9)$$

where k_{SR} and k_{PBR} are the rate constants for the surface and phase boundary reactions, respectively. Differently, the similar $T-\alpha$ profile of CRTA observed for the thermal decomposition of $\text{Na}_2\text{CO}_3 \cdot (3/2)\text{H}_2\text{O}_2$ was interpreted by a physico-geometrical model that assumes the acceleration of linear advancement rate of reaction interface in the scheme of contracting geometry [36]. This type of reaction also indicates a sigmoidal shape of the integral kinetic curve ($\alpha-t$) under isothermal conditions and expressed by the kinetic model function originally proposed by Galwey and Hood [117].

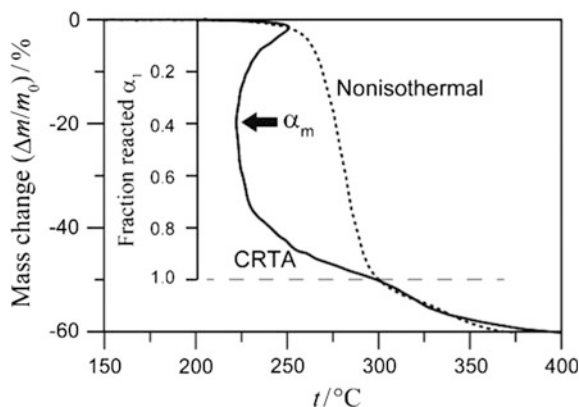
$$f(\alpha) = 2n(1-\alpha)^{1-1/n} \left[1 - (1-\alpha)^{1/n} \right]^{1/2} \quad (2.10)$$

where n is the dimension of interface shrinkage. Many other examples of the successful use of SCTA and CRTA for the study of kinetics and mechanisms of solid-state reaction can be found in literatures [10, 13, 22, 50, 61, 63, 118–144], which involve the kinetic studies of solid–gas reactions in the framework of the CO₂ capture from the atmosphere [136, 137].

SCTA methods have also been applied to the thermal degradation of polymers [84, 103, 145–154]. The T – α profile of CRTA for the typical reaction mechanism of polymer degradation known as the random scission mechanism is similar to those of Am models [103, 149]. The reaction mechanism of the thermal degradation of polybutylene (PBT) has been characterized as a random scission of the polymer chains using CRTA [146]. Another example of the polymer degradation studied using CRTA is for polyvinyl chloride (PVC). In many previous studies that used the conventional thermal analysis [155–160], F1 model has been selected as the most appropriate kinetic model for the dehydrochlorination reaction. However, the α – T profile of CRTA does not fit to F1 model as shown in Fig. 2.9 [11, 146] and clearly indicate the two-step feature of the process, which cannot be deconvoluted in the conventional linear nonisothermal method. The α – T profile of CRTA for the first reaction step is characterized by the appearance of the minimum temperature midway through the reaction. Therefore, the reaction mechanism of the first reaction step of the thermal dehydrochlorination of PVC can be interpreted either by an Am model [11, 146] or a random scission model [150].

The potential of CRTA for the kinetic model discrimination would be approved by the above review. Once the appropriate kinetic model function was selected from a single CRTA curve through the shape analysis of T – α profile of CRTA and using available master plot methods, the Arrhenius parameters can separately be determined based on Eq. (2.1) from the same CRTA curve [85, 161]. In addition, the reliability of the calculated Arrhenius parameters can be confirmed by the comparison with the E_a value determined using the rate jump CRTA method [65–67]. Therefore, two CRTA measurements, one is the ordinal and the other is the rate jump measurements, are the minimum requirement for the kinetic analysis. Of

Fig. 2.9 Comparison of mass-change traces for the thermal dehydrochlorination of PVC recorded under linear nonisothermal condition at $\beta = 2 \text{ K min}^{-1}$ and CRTA condition at $C (= d\alpha/dt) = 5 \times 10^{-4} \text{ s}^{-1}$ [11, 84, 146]



course, a systematic kinetic approach with the measurements of a series of CRTA curves under different measurement conditions of m_0 or C are preferable. Using the series of CRTA curves, the recommended two-step kinetic analysis, determination of E_a by the isoconversional method and the subsequent analysis of the experimental master plot for determining $f(\alpha)$ and A , can be performed using the universally applicable procedures of kinetic calculation [28, 34, 80–82].

2.4 Application of SCTA to Material Synthesis

2.4.1 Controls of Porosity and Specific Surface Area

The potential of SCTA to control the self-generated reaction conditions in a sophisticated manner can be applied to the synthetic reactions of materials. The application of SCTA to material synthesis was first attempted by Rouquerol et al. [162, 163] for the thermal decomposition of $\text{Al}(\text{OH})_3$ (gibbsite) crystals to form Al_2O_3 , where the influence of partial pressure of the self-generated water vapour on the variation of specific area of reacting sample was examined using CRTA under vacuum. The thermal decomposition process was controlled at a constant decomposition rate C ($= \text{d}x/\text{d}t$) of $5.5 \times 10^{-4} \text{ min}^{-1}$ under different residual pressures of water vapour within the range from 5.3 to 667 Pa. As shown in Fig. 2.10a, the variation of specific surface area of the reacting sample largely depends on the residual pressure of water vapour, where the initial increase in the specific surface area dramatically increases with increasing the residual pressure. The maximum value of the specific surface area attained during the thermal decomposition varied from $40 \text{ m}^2 \text{ g}^{-1}$ at 5.3 Pa up to $450 \text{ m}^2 \text{ g}^{-1}$ at 667 Pa. On further heating, the specific surface area turns to decrease at the temperature in the range of 250–300 °C irrespective of the residual pressure. The diminution of the specific surface also depends on the residual pressure, indicating the higher the residual pressure is the lower the decrease degree. As the results, the final product of Al_2O_3 with the larger specific surface area was obtained when the sample was decomposed at a constant reaction rate under higher residual pressure of water vapour. The phenomena were lately reconfirmed by Stacey [164, 165] and Barnes and Parkes [166] for the thermal decompositions of $\text{Al}(\text{OH})_3$ (gibbsite) and $\text{AlO}(\text{OH})$ (boehmite) and explained with experimental evidence of the formations of slit-shaped micropores, mesopores, and macropores and the variations of those contributions to the specific surface area depending on the residual pressure of water vapour during the course of reaction. With decreasing the residual pressure, the specific surface area attributed to the microporosity increases accompanied with a decrease in the width of the slit pores, while the specific surface area attributed to mesoporosity and macroporosity decreases. The significant low specific surface area when the thermal decomposition was subjected under lower residual pressure was interpreted by the formation of slit pores with narrow width that cannot be accessed by nitrogen during the measurement of specific surface area using the Brunauer–Emmett–Teller

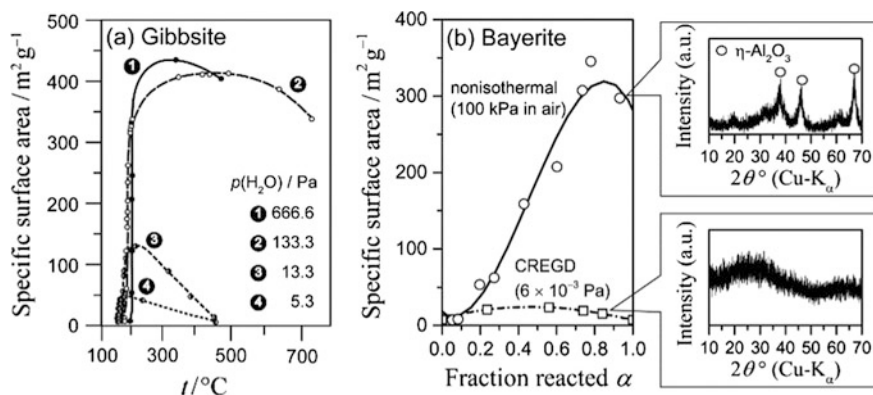


Fig. 2.10 Variation of the specific surface area during the thermal decompositions of $\text{Al}(\text{OH})_3$: **a** gibbsite (grain size 1 μm) at a constant reaction rate $C (= \text{d}\alpha/\text{d}t)$ of $5.5 \times 10^{-4} \text{ min}^{-1}$ under different water vapour pressures [162] and **b** bayerite ($m_0 = 300 \text{ mg}$) under linear heating condition at $\beta = 2 \text{ K min}^{-1}$ in air and under CRTA at a controlled water vapour pressure of $6.0 \times 10^{-3} \text{ Pa}$ ($C = 18.4 \mu\text{g min}^{-1}$), together with the powder XRD patterns of the product solids [138, 167]

(BET) method. The decrease in the specific surface area on further heating the sample at a temperature higher than 300 °C has been explained by the effective annealing temperature for the microporosity being lower than that of mesopores and macropores. A comparison of the changes in the specific surface area during the thermal decomposition of synthetic bayerite ($\text{Al}(\text{OH})_3$) under linear heating condition in air (100 kPa) and under CRTA condition of controlled residual pressure at $6.0 \times 10^{-3} \text{ Pa}$ also indicated the lower maximum specific surface area under the CRTA condition in reduced pressure (Fig. 2.10b), where the maximum specific surface area of each process was approximately $350 \text{ m}^2 \text{ g}^{-1}$ at $\alpha = 0.9$ and $25 \text{ m}^2 \text{ g}^{-1}$ at $\alpha = 0.4$ under the linear heating condition and the CRTA condition, respectively [138, 167]. $\eta\text{-Al}_2\text{O}_3$ was obtained as the decomposition product under the linear heating condition, while the product was amorphous to XRD under the CRTA condition.

Possible control of porosity of reacting sample during the thermal decomposition of solids under vacuum was also demonstrated by controlling the decomposition rate and residual pressure of water vapour for the thermal decomposition of $\alpha\text{-FeO}(\text{OH})$ (goethite to form $\alpha\text{-Fe}_2\text{O}_3$ (hematite) [168, 169], in which an independent control of both constant reaction rate and constant residual pressure of water vapour was applied using SCTA. By the SCTA control under vacuum, the porosity of the hematite product can be controlled by the formations of two different types of pore structures as shown in Fig. 2.11. Those are the isolated round pores formed at higher residual pressures (Fig. 2.11a) and slit pore channels oriented along the c -lattice axis (the long axis of the particle) formed at very low water vapour pressures (Fig. 2.11b). The specific surface area of the produced hematite was significantly increased with decreasing the controlled residual pressure of water vapour during

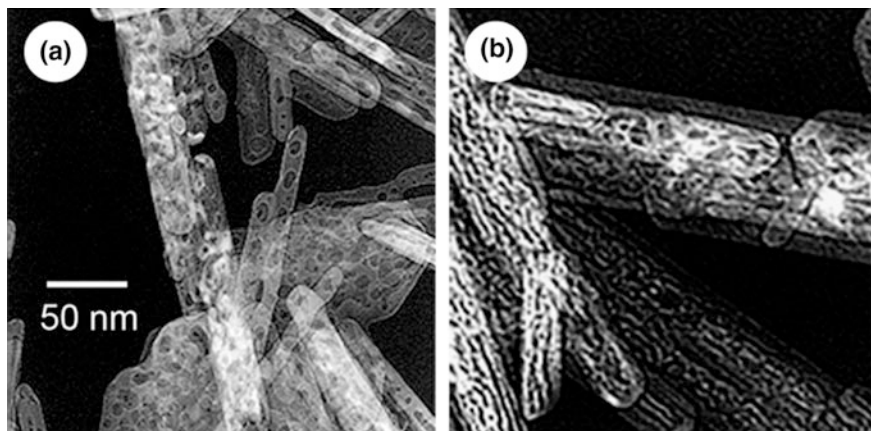


Fig. 2.11 TEM micrographs of the hematite products obtained by the thermal decomposition of goethite under CRTA conditions: **a** $P = 1.1 \text{ kPa}$ and $C = 7.6 \times 10^{-4} \text{ min}^{-1}$ and **b** $P = 7.3 \times 10^{-3} \text{ Pa}$ and $C = 3.3 \times 10^{-3} \text{ min}^{-1}$ [168, 169]

the thermal decomposition of goethite [168, 169]. A similar behaviour was also found for the thermal decomposition of $\gamma\text{-FeOOH}$ (lepidocrocite) to form $\gamma\text{-Fe}_2\text{O}_3$ (maghemite) when both the rate and the water vapour pressure were controlled during the thermal decomposition using CRTA [170]. However, the trend of the residual pressure-specific surface area relationship observed for the thermal decomposition of goethite and lepidocrocite is apparently opposite to those described above for the thermal decompositions of gibbsite, bayerite, and hematite, although the respective hydroxides and oxyhydroxides have the similar crystal structures. It is noteworthy to point out that the microporosity increases in both isostructural oxyhydroxides by decreasing the water partial pressure during the dehydroxylation reaction, but the size of the slit-shaped microporous generated from iron oxyhydroxides are larger than those generated from aluminium oxyhydroxides; therefore, they are accessible to the nitrogen adsorption. This behaviour would explain that the BET surface of iron oxides obtained from the dehydration of oxyhydroxides increases by increasing the microporosity, contrarily what occurs in the case of the alumina obtained from aluminium oxyhydroxide. The size of the structural microporous generated during the dehydroxylation of these compounds perhaps would be controlled by the cation size in such a way that the lower is the cation radius the lower is the size of the microporous.

The potential of SCTA for controlling the porosity and specific surface area of the oxides produced by the thermal decomposition of precursor compounds under controlled vacuum and reaction rate can be applicable to the syntheses of adsorbents and catalysts as have been reported in many works [113, 124, 171–177]. Those works have previously been reviewed by Llewellyn et al. [178], Fesenko et al. [114], and Pérez-Maqueda et al. [179].

2.4.2 Controls of Particle Morphology, Size, and Phase Composition

The SCTA control of both the residual pressure under dynamic vacuum and the reaction rate has also been applied to the synthesis of barium titanate (BaTiO_3) from the thermal decomposition of its oxalate and citrate precursors [180–183] and it was reported the successful controls of particle morphology, particle size, and phase composition of BaTiO_3 polymorphs. The crystal size and the stabilization of the cubic phase with regards to the tetragonal phase of BaTiO_3 were controlled by changing the controlled residual pressure to different constant values in the range from 10^{-2} Pa to 10 kPa, in which the crystal size of BaTiO_3 was decreased and the cubic phase was stabilized by decreasing the constant residual pressure. Figure 2.12 shows the electron microscopic views of the citrate precursor (Fig. 2.12a) and BaTiO_3 products (Fig. 2.12b–d). Round powder particles of BaTiO_3 were obtained by the conventional isothermal annealing treatment (Fig. 2.12b). Under some selected conditions of constant residual pressure and reaction rate using CRTA method, BaTiO_3 fibres constituted by welded nanocrystals (Fig. 2.12c, d) were obtained through the thermal decomposition of acicular shaped particles of barium titanyl citrate [184].

A successful control of the phase composition and the crystal and particle sizes has also been reported for the synthesis of Si_3N_4 through the carbothermal nitridization of silica using SCTA by controlling both the reaction rate and the partial pressure of CO generated by the carbothermal reduction of silica [185–187]. Figure 2.13 compares the SEM images of two Si_3N_4 products obtained through the carbothermal reduction of silica in flowing a mixed $\text{N}_2\text{--H}_2$ gas (95% N_2) and by controlling the reaction rate to be constant at $C (= d\alpha/dt)$ of $1.1 \times 10^{-3} \text{ min}^{-1}$ under different controlled partial pressures of CO generated by the carbothermal reduction of silica, which was subsequently annealed isothermally at 1450 °C for 5 h in flowing the mixed gas [187]. The Si_3N_4 produced by the thermal decomposition at the lowest constant residual concentration of CO is constituted by a mixture of $\beta\text{-Si}_3\text{N}_4$ ribbons and small hexagonal crystallites of $\alpha\text{-Si}_3\text{N}_4$ (Fig. 2.13a), while that obtained at the higher residual CO concentration is constituted by hexagonal crystallites of pure $\alpha\text{-Si}_3\text{N}_4$ with homogeneous size (Fig. 2.13b). The application of SCTA to the synthesis of other ceramic materials has also been reported [188–193].

2.4.3 Controls of Debinding and Curing Processes

Multilayer capacitors (MLCs) or in general multilayer actuators (MLAs) constituted by layers of ferroelectric ceramics separated by electrode metal layers are manufactured by stacking the different layers by a tape casting technology, generally using an organic binder, followed by debinding and sintering processes by co-firing

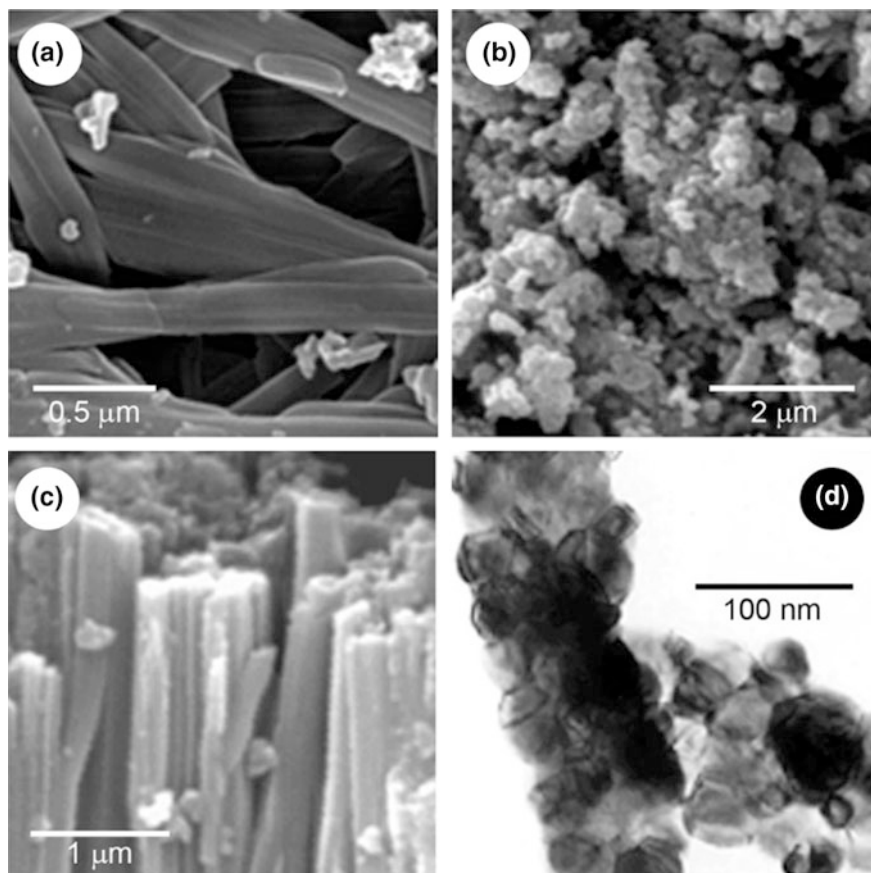


Fig. 2.12 Electron microscopic views of the citrate precursor and its thermal decomposition product, BaTiO_3 : **a** barium titanyl citrate (SEM); **b** BaTiO_3 obtained by isothermal annealing at 700 °C for 5 h (SEM). **c** BaTiO_3 obtained by the thermal treatment under CRTA conditions ($P = 1.3 \times 10^{-3}$ Pa) and subsequent isothermal annealing at 700 °C for 5 h (SEM) **d** as in (c) (TEM) [184]

treatment. The possible crack formation during the co-firing treatment is the main problem in the manufacturing of these devices. Therefore, the debinding process is a rather cumbersome process that very often takes several weeks [194]. The control of debinding rate at a low constant rate using SCTA is one of the possible solutions for avoiding the crack formation as demonstrated by Speyer et al. [194, 195]. Figure 2.14 illustrates the optical microscopic views of the polished surfaces of MLAs obtained by debinding at different controlled rates. It is clearly shown that the delaminating damage is dramatically reduced by decreasing the debinding rate.

The SCTA technique has also been applied to the thermal curing of concretes [196]. During the curing process, crystallization of xonotlite and other hydrates can be hindered by the control of the thermal dehydration rate at a low constant rate and

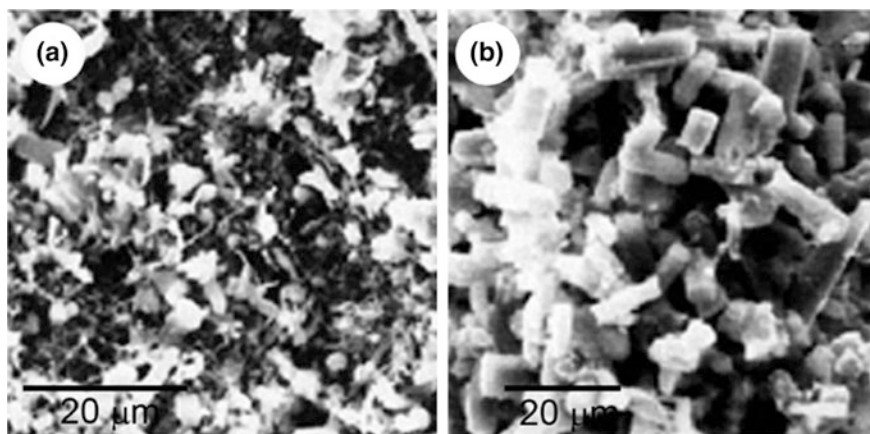


Fig. 2.13 SEM images of Si_3N_4 obtained from carbothermal reduction of silica at the constant reaction rate C ($= dz/dt$) of $1.1 \times 10^{-3} \text{ min}^{-1}$ under different constant concentration of CO : **a** 20 Pa and **b** 1 kPa [187]

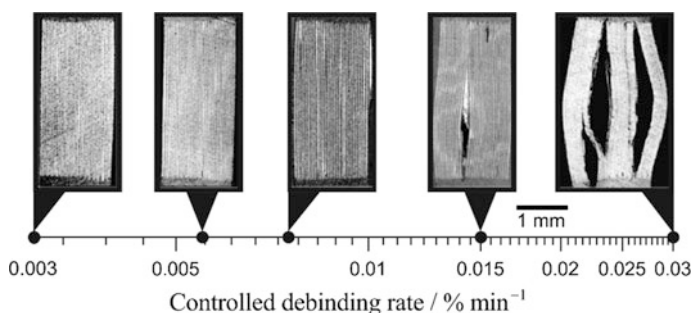


Fig. 2.14 Optical microscopic views of the polished surfaces of MLAs obtained under different controlled debinding rates [195]

maintain the partial pressure of water vapour in the close vicinity of the samples at a lower value. SCTA techniques were also useful for controlling the interfibre porosity and for eliminating the structural microporosity of sepiolites [197] and for synthesising oxide systems with tailored specific surface [198–200]. A study of the thermal dehydration of the hydrated rare earth polyphosphates using SCTA for obtaining the anhydrous salts, which is of great interest as catalysts and luminescent materials, has been reported in literature [201, 202]. A novel $\text{Ce}(\text{PO}_3)_3$ phase with a crystal structure, different from those of the other lanthanide polyphosphates, has been obtained by controlling the thermal dehydration at a constant reaction rate so as to maintain the partial pressure of self-generated water vapour to be a constant value of 5 kPa [201].

2.5 Conclusions

In addition to the higher resolution power for the thermally induced multistep processes, SCTA techniques represent higher potentials for applying to the kinetic analysis of the solid-state reactions and polymer degradations and for controlling the synthetic and manufacturing processes of materials and devices. The special performance of SCTA to control the reaction rate at a small constant value and the partial pressure of the evolved gas at a low constant value offers the measurements of the kinetic rate data for the reaction under the controlled reaction conditions involving the conditions self-generated by the reaction itself. In modern SCTA instruments, the reaction rate is controlled precisely even for the process with a small total change of the measured physical properties, for example several hundred μg in TG. The SCTA measurement using a small amount sample provides ideal kinetic rate data, in which the gradients in temperature and partial pressure within the sample matrix are largely diminished in comparison with conventional isothermal and linear nonisothermal measurements. When applying the data to kinetic calculation, the $T-\alpha$ profile of CRTA are characteristic for the respective kinetic models; therefore, the appropriate kinetic model function can easily be estimated using available master plot methods. This is the significant merit to avoid possible distortions of the calculated Arrhenius parameters by the wrong choice of the kinetic model function. In applying SCTA for material synthesis processes, both the reaction rate and the partial pressure of gases can be controlled to be different constant values in wide ranges by changing the applied reaction atmosphere, pumping rate to vacuum, sample mass, controlled transformation rate, and so on. The performance of SCTA can be used for obtaining the solid products with the desired chemical and physical properties in the more sophisticated manner in comparison with the empirical annealing treatments. The advantages of SCTA have been evidenced by the previous works reviewed in this chapter, and the techniques can further contribute to the promising advancement of modern material sciences.

References

1. Smith CS (1940) A simple method of thermal analysis permitting quantitative measurements of specific and latent heats. *Trans AIME* 137:236–245
2. Charsley EL, Laye PG, Parkes GMB, Rooney JJ (2010) Development and applications of a sample controlled DSC system. *J Therm Anal Calorim* 105(2):699–703
3. Saccone A, Macciò D, Robinson JAJ, Hayes FH, Ferro R (2001) Smith thermal analysis of selected Pr–Mg alloys. *J Alloys Compd* 317–318:497–502
4. Rouquerol J (1970) L'analyse thermique a vitesse de decomposition constante. *J Therm Anal* 2(2):123–140
5. Rouquerol J (1997) Controlled rate evolved gas analysis: 35 years of rewarding services. *Thermochim Acta* 300(1–2):247–253
6. Rouquerol J (1964) Methode d'analyse thermique sous faible pression et a vitesse de decomposition constante. *Bull Soc Chim Fr*:31–32

7. Paulik J, Paulik F (1971) "Quasi-isothermal" thermogravimetry. *Anal Chim Acta* 56(2):328–331
8. Paulik F, Paulik J (1986) Thermoanalytical examination under quasi-isothermal—quasi-isobaric conditions. *Thermochim Acta* 100(1):23–59
9. Paulik F (1999) Thermal analysis under quasi-isothermal–quasi-isobaric conditions. *Thermochim Acta* 340–341:105–116
10. Barnes PA, Parkes GMB, Charsley EL (1994) High-performance evolved gas analysis system for catalyst characterization. *Anal Chem* 66(14):2226–2231
11. Diáñez MJ, Pérez-Maqueda LA, Criado JM (2004) Direct use of the mass output of a thermobalance for controlling the reaction rate of solid-state reactions. *Rev Sci Instrum* 75(8):2620–2624
12. Criado JM, Pérez-Maqueda LA, Diáñez MJ, Sánchez-Jiménez PE (2007) Development of a universal constant rate thermal analysis system for being used with any thermoanalytical instrument. *J Therm Anal Calorim* 87(1):297–300
13. Koga N, Yamada S (2005) Influences of product gases on the kinetics of thermal decomposition of synthetic malachite evaluated by controlled rate evolved gas analysis coupled with thermogravimetry. *Int J Chem Kinet* 37(6):346–3549
14. Sørensen OT (1981) Quasi-isothermal methods in thermal analysis. *Thermochim Acta* 50(1–3):163–175
15. Parkes GMB, Barnes PA, Charsley EL (1998) Gas concentration programming—a new approach to sample controlled thermal analysis. *Thermochim Acta* 320(1–2):297–301
16. Ortega A, Pérez-Maqueda LA, Criado JM (1994) Simultaneous determination of the activation energy and the reaction kinetic model from the analysis of a single curve obtained by a novel method. *J Therm Anal* 42(2–3):551–557
17. Ortega A, Pérez-Maqueda LA, Criado JM (1994) Shape analysis of the α -T curves obtained by CRTA with constant acceleration of the transformation. *Thermochim Acta* 239:171–180
18. Gill PS, Sauerbrunn SR, Crowe BS (1992) High resolution thermogravimetry. *J Therm Anal* 38(3):255–266
19. Sánchez-Jiménez PE, Pérez-Maqueda LA, Crespo-Amoros JE, Lopez J, Perejon A, Criado JM (2010) Quantitative characterization of multicomponent polymers by sample-controlled thermal analysis. *Anal Chem* 82(21):8875–8880
20. Wang FC-Y (2000) Polymer additive analysis by pyrolysis–gas chromatography. *J Chromatogr A* 891(2):325–336
21. Peris-Vicente J, Baumer U, Stege H, Lutzenberger K, Gimeno Adelantado JV (2009) Characterization of commercial synthetic resins by pyrolysis-gas chromatography/mass spectrometry: application to modern art and conservation. *Anal Chem* 81(8):3180–3187
22. Pérez-Maqueda LA, Criado JM, Sánchez-Jiménez PE, Perejón A (2013) Kinetic studies in solid state reactions by sample-controlled methods and advanced analysis procedures. *J Therm Anal Calorim* 113(3):1447–1453
23. Koga N (2015) Kinetic characterization of the inorganic solid-state reactions using thermal analysis. *Netsu Sokutei* 42(1):2–9
24. Koga N, Šesták J, Simon P (2013) Some fundamental and historical aspects of phenomenological kinetics in the solid state studied by thermal analysis. In: Šesták J, Simon P (eds) *Thermal analysis of micro, nano- and non-crystalline materials*. Springer, Berlin, pp 1–28
25. Koga N (2013) Ozawa's kinetic method for analyzing thermoanalytical curves. *J Therm Anal Calorim* 113(3):1527–1541
26. Koga N, Tanaka H (2002) A physico-geometric approach to the kinetics of solid-state reactions as exemplified by the thermal dehydration and decomposition of inorganic solids. *Thermochim Acta* 388(1–2):41–61
27. Khawam A, Flanagan DR (2006) Basics and applications of solid-state kinetics: a pharmaceutical perspective. *J Pharm Sci* 95(3):472–498

28. Vyazovkin S, Burnham AK, Criado JM, Pérez-Maqueda LA, Popescu C, Sbirrazzuoli N (2011) ICTAC Kinetics Committee recommendations for performing kinetic computations on thermal analysis data. *Thermochim Acta* 520(1–2):1–19
29. Vyazovkin S, Chrissafis K, Di Lorenzo ML, Koga N, Pijolat M, Roduit B, Sbirrazzuoli N, Suñol JJ (2014) ICTAC kinetics committee recommendations for collecting experimental thermal analysis data for kinetic computations. *Thermochim Acta* 590:1–23
30. Koga N, Maruta S, Kimura T, Yamada S (2011) Phenomenological kinetics of the thermal decomposition of sodium hydrogencarbonate. *J Phys Chem A* 115(50):14417–14429
31. Reading M (1992) Controlled rate thermal analysis and beyond. In: Charsley EL, Warrington SB (eds) *Thermal analysis-techniques and applications*. Royal Society of Chemistry, Cambridge, pp 126–155
32. Reading M (1998) Controlled rate thermal analysis and related techniques. In: Brown ME (ed) *Handbook of thermal analysis and calorimetry*, vol 1. Elsevier, Amsterdam, pp 423–443
33. Ozawa T (1986) Applicability of Friedman plot. *J Therm Anal* 31:547–551
34. Koga N (1995) Kinetic analysis of thermoanalytical data by extrapolating to infinite temperature. *Thermochim Acta* 258:145–159
35. Koga N, Kimizu T (2008) Thermal decomposition of indium(III) hydroxide prepared by the microwave-assisted hydrothermal method. *J Am Ceram Soc* 91(12):4052–4058
36. Wada T, Koga N (2013) Kinetics and mechanism of the thermal decomposition of sodium percarbonate: role of the surface product layer. *J Phys Chem A* 117(9):1880–1889
37. Friedman HL (1964) Kinetics of thermal degradation of cha-forming plastics from thermogravimetry. Application to a phenolic plastic. *J Polym Sci C* 6:183–195
38. Garner WE (1955) *Chemistry of the solid state*. Butterworths, London
39. Criado JM, Rouquerol F, Rouquerol J (1980) Thermal decomposition reactions in solids—comparison of the constant decomposition rate thermal analysis with the conventional TG method. *Thermochim Acta* 38(1):109–115
40. Criado JM (1980) Study of the thermal decomposition of double strontium and barium carbonates using a new technique: constant rate thermal analysis (CRTA). *Mater Sci Monogr* 6:1096–2001
41. Criado JM (1982) Determination of the mechanism of thermal decomposition of MnCO_3 , CdCO_3 , and PbCO_3 by using the TG and the cyclic and constant decomposition rate of thermal analysis. In: Miller B (ed) *Thermal analysis, The 7th international conference on thermal analysis, 1982*. Wiley, pp 99–105
42. Reading M, Dollimore D, Rouquerol J, Rouquerol F (1984) The measurement of meaningful activation energies. *J Therm Anal* 29(4):775–785
43. Criado JM, Ortega A, Rouquerol J, Rouquerol F (1987) A new method of thermal analysis: thermal analysis under controlled rate. II Kinetic analysis. *Bol Soc Esp Cerám* 25:3–11
44. Ortega A, Akhouayri S, Rouquerol F, Rouquerol J (1990) On the suitability of controlled transformation rate thermal analysis (CRTA) for kinetic studies. *Thermochim Acta* 163:25–32
45. Criado JM, Dıanez MJ, Macias M, Paradas MC (1990) Crystalline structure and thermal stability of double strontium and barium carbonates. *Thermochim Acta* 171:229–238
46. Reading M, Dollimore D, Whitehead R (1991) The measurement of meaningful kinetic parameters for solid state decomposition reactions. *J Therm Anal* 37(9):2165–2188
47. Criado JM, Ortega A (1991) Kinetic study of thermal decomposition of dolomite by controlled transformation rate thermal analysis (CRTA) and TG. *J Therm Anal* 37(10):2369–2375
48. Málek J, Šesták J, Rouquerol F, Rouquerol J, Criado JM, Ortega A (1992) Possibilities of two non-isothermal procedures (temperature- or rate-controlled) for kinetical studies. *J Therm Anal* 38(1–2):71–87
49. Ortega A, Akhouayri S, Rouquerol F, Rouquerol J (1994) On the suitability of controlled transformation rate thermal analysis (CRTA) for kinetic studies. Part 3. Discrimination of the reaction mechanism of dolomite thermolysis. *Thermochim Acta* 247(2):321–327

50. Laureiro Y, Jerez A, Rouquérol F, Rouquérol J (1996) Dehydration kinetics of Wyoming montmorillonite studied by controlled transformation rate thermal analysis. *Thermochim Acta* 278:165–173
51. Koga N, Criado JM (1998) The influence of mass transfer phenomena on the kinetic analysis for the thermal decomposition of calcium carbonate by constant rate thermal analysis (CRTA) under vacuum. *Int J Chem Kinet* 30(10):737–744
52. Hatakeyama T, Zhenhai L (1998) *Handbook of thermal analysis*. Wiley, Chichester
53. Finaru A, Salageanu I, Segal E (2000) Non-isothermal kinetic study of the heterogeneous thermal decomposition of a Mannich compound. *J Therm Anal Calorim* 61(1):239–242
54. Koga N, Criado JM, Tanaka H (2000) Kinetic analysis of inorganic solid-state reactions by controlled rate thermal analysis. *Netsu Sokutei* 27(3):128–140
55. Criado JM, Ortega A, Rouquerol J, Rouquerol F (1994) Influence of pressure on the shape of TG and controlled transformation rate thermal analysis (CRTA) traces. *Thermochim Acta* 240:247–256
56. Criado J, González M, Málek J, Ortega A (1995) The effect of the CO₂ pressure on the thermal decomposition kinetics of calcium carbonate. *Thermochim Acta* 254:121–127
57. Rouquerol F, Laureiro Y, Rouquerol J (1993) Influence of water vapour pressure on the thermal dehydration of lithium sulphate monohydrate. *Solid State Ionics* 63–65:363–366
58. Bordère S, Rouquérol F, Llewellyn PL, Rouquérol J (1996) Unexpected effect of pressure on the dehydration kinetics of uranyl nitrate trihydrate: an example of a Smith-Topley effect. *Thermochim Acta* 282–283:1–11
59. Pérez-Maqueda LA, Criado JM, Gotor FJ (2002) Controlled rate thermal analysis commanded by mass spectrometry for studying the kinetics of thermal decomposition of very stable solids. *Int J Chem Kinet* 34(3):184–192
60. Koga N, Criado JM, Tanaka H (1999) Apparent kinetic behavior of the thermal decomposition of synthetic malachite. *Thermochim Acta* 340–341:387–394
61. Yamada S, Koga N (2005) Kinetics of the thermal decomposition of sodium hydrogen carbonate evaluated by controlled rate evolved gas analysis coupled with thermogravimetry. *Thermochim Acta* 431(1–2):38–43
62. Koga N, Criado JM, Tanaka H (2000) Kinetic analysis of the thermal decomposition of synthetic malachite by CRTA. *J Therm Anal Calorim* 60(3):943–954
63. Yamada S, Tsukumo E, Koga N (2009) Influences of evolved gases on the thermal decomposition of zinc carbonate hydroxide evaluated by controlled rate evolved gas analysis coupled with TG. *J Therm Anal Calorim* 95(2):489–493
64. Paulik F (1995) *Special trends in thermal analysis*. Wiley, Chichester
65. Rouquerol J (1985) Recent developments in the calorimetric and thermoanalytical approaches to problems related to fossil-fuels (genesis, extraction and use). *Pure Appl Chem* 57(1):69–77
66. Rouquerol F, Rouquerol J (1971) Activation energy of a thermolysis: conditions for significant measurements under very low pressure. In: Wiedemann HG (ed) *Thermal analysis, Proceedings of the 3rd international conference on thermal analysis*, Davos, 1971. Birkhauser Verlag, pp 373–377
67. Rouquerol F, Regnier S, Rouquerol J (1975) Activation energy of the dehydration of a silica gel between 200 and 1000 °C. In: Buzas I (ed) *Thermal analysis, Proceedings of the 4th international conference on thermal analysis*, Budapest, 1975, vol 1. Akademiai Kiadó and Heyden & Sons, pp 313–318
68. Reading M (1988) The kinetics of heterogeneous solid state decomposition reactions. *Thermochim Acta* 135:37–57
69. Sørensen OT, Rouquerol J (2003) *Sample controlled thermal analysis: origin, goals, multiple forms, applications and future*. Kluwer, Dordrecht
70. Koga N (1994) A review of the mutual dependence of Arrhenius parameters evaluated by the thermoanalytical study of solid-state reactions: the kinetic compensation effect. *Thermochim Acta* 244(1):1–20

71. Criado JM, Ortega A, Gotor FJ (1990) Correlation between the shape of controlled-rate thermal analysis curves and the kinetics of solid-state reactions. *Thermochim Acta* 157:171–179
72. Criado JM, Pérez-Maqueda LA (2003) SCTA and kinetics. In: Sørensen OT, Rouquerol J (eds) *Sample controlled thermal analysis: origin, goals, multiple forms, applications and future*. Kluwer, Dordrecht, pp 62–101
73. Criado JM, Gonzalez M (1981) The method of calculation of kinetic parameters as a possible cause of apparent compensation effects. *Thermochim Acta* 46(2):201–207
74. Tanaka H, Koga N (1988) Kinetic compensation effect between the isothermal and non-isothermal decomposition of solids. *J Therm Anal* 34(3):685–691
75. Koga N, Tanaka H (1991) A kinetic compensation effect established for the thermal-decomposition of a solid. *J Therm Anal* 37(2):347–363
76. Koga N, Šesták J (1991) Kinetic compensation effect as a mathematical consequence of the exponential rate-constant. *Thermochim Acta* 182(2):201–208
77. Koga N, Šesták J (1991) Further aspects of the kinetic compensation effect. *J Therm Anal* 37(5):1103–1108
78. Koga N, Šesták J, Málek J (1991) Distortion of the Arrhenius parameters by the inappropriate kinetic-model function. *Thermochim Acta* 188(2):333–336
79. Málek J, Criado JM (1992) Empirical kinetic models in thermal analysis. *Thermochim Acta* 203:25–30
80. Málek J (1992) The kinetic analysis of non-isothermal data. *Thermochim Acta* 200:257–269
81. Gotor FJ, Criado JM, Málek J, Koga N (2000) Kinetic analysis of solid-state reactions: the universality of master plots for analyzing isothermal and nonisothermal experiments. *J Phys Chem A* 104(46):10777–10782
82. Criado JM, Pérez-Maqueda LA, Gotor FJ, Malek J, Koga N (2003) A unified theory for the kinetic analysis of solid state reactions under any thermal pathway. *J Therm Anal Calorim* 72(3):901–906
83. Pérez-Maqueda LA, Criado JM, Sánchez-Jiménez PE (2006) Combined kinetic analysis of solid-state reactions: a powerful tool for the simultaneous determination of kinetic parameters and the kinetic model without previous assumptions on the reaction mechanism. *J Phys Chem A* 110(45):12456–12462
84. Pérez-Maqueda LA, Criado JM, Sánchez-Jiménez PE, Diáñez MJ (2015) Applications of sample-controlled thermal analysis (SCTA) to kinetic analysis and synthesis of materials. *J Therm Anal Calorim* 120(1):45–51
85. Criado JM (1979) On the kinetic analysis of thermoanalytical diagrams obtained with the “quasi-isothermal” heating technique. *Thermochim Acta* 28(2):307–312
86. Criado JM, Morales J (1976) Defects of thermogravimetric analysis for discerning between first order reactions and those taking place through the Avrami-Erofeev’s mechanism. *Thermochim Acta* 16:382–387
87. Criado JM, Morales J (1980) On the evaluation of kinetic parameters from thermogravimetric curves. *Thermochim Acta* 41(1):125–127
88. Criado JM, Dollimore D, Heal GR (1982) A critical study of the suitability of the Freeman and Carroll method for the kinetic analysis of reactions of thermal decomposition of solids. *Thermochim Acta* 54(1–2):159–165
89. Flynn JH (1988) Thermal analysis kinetics—problems, pitfalls and how to deal with them. *J Therm Anal* 34(1):367–381
90. Agrawal RK (1988) Analysis of irreversible complex chemical reactions and some observations on their overall activation energy. *Thermochim Acta* 128:185–208
91. Vyazovkin S, Wight CA (1998) Isothermal and non-isothermal kinetics of thermally stimulated reactions of solids. *Int Rev Phys Chem* 17(3):407–433
92. Vyazovkin SV, Lesnikovich AI (1989) On the methods of solving the inverse problem of solid-phase reaction kinetics. *J Therm Anal* 35(7):2169–2188
93. Brown ME, Maciejewski M, Vyazovkin S, Nomen R, Sempere J, Opfermann J, Strej R, Anderson HL, Kemmler A, Keuleers R, Janssens J, Desseyn HO, Li C-R, Tang TB,

- Roduit B, Malek J, Mitsuhashi T (2000) Computational aspects of kinetic analysis. *Thermochim Acta* 355(1–2):125–143
94. Pérez-Maqueda LA, Ortega A, Criado JM (1996) The use of master plots for discriminating the kinetic model of solid state reactions from a single constant-rate thermal analysis (CRTA) experiment. *Thermochim Acta* 277:165–173
95. Koga N, Criado JM (1997) Influence of the particle size distribution on the CRTA curves for the solid-state reactions of interface shrinkage. *J Therm Anal* 49(3):1477–1484
96. Koga N, Criado JM (1998) Kinetic analyses of solid-state reactions with a particle-size distribution. *J Am Ceram Soc* 81(11):2901–2909
97. Criado JM (1981) On the determination of the activation energy of solid-state reactions from the maximum reaction rate of isothermal runs. *J Therm Anal* 21(1):155–157
98. Tiernan MJ, Barnes PA, Parkes GMB (2001) Reduction of iron oxide catalysts: the investigation of kinetic parameters using rate perturbation and linear heating thermoanalytical techniques. *J Phys Chem B* 105(1):220–228
99. Mampel KL (1940) Time conversion formulas for heterogeneous reactions at the phase boundaries of solid bodies I: the development of the mathematical method and the derivation of area conversion formulas. *Z Phys Chem A* 187:43–57
100. Prout EG, Tompkins FC (1944) The thermal decomposition of potassium permanganate. *Trans Faraday Soc* 40:488–497
101. Prout EG, Tompkins FC (1946) The thermal decomposition of silver permanganate. *Trans Faraday Soc* 42(6–7):468–472
102. Simha R, Wall LA (1952) Kinetics of chain depolymerization. *J Phys Chem* 56(6):707–715
103. Sánchez-Jiménez PE, Pérez-Maqueda LA, Perejón A, Criado JM (2010) A new model for the kinetic analysis of thermal degradation of polymers driven by random scission. *Polym Degrad Stab* 95(5):733–739
104. Criado JM, Ortega A, Real C (1987) Mechanism of the thermal decomposition of anhydrous nickel nitrate. *React Solids* 4:93–103
105. Paulik J, Paulik F (1981) Simultaneous thermoanalytical examinations by means of derivatograph. Wilson-Wilson's *Comprehensive Analytical Chemistry*, vol XII. Elsevier, Amsterdam
106. Barnes PA, Parkes GMB, Brown DR, Charsley EL (1995) Applications of new high resolution evolved-gas analysis systems for the characterisation of catalysts using rate-controlled thermal analysis. *Thermochim Acta* 269–270:665–676
107. Gomez F, Vast P, Llewellyn P, Rouquerol F (1997) Dehydroxylation mechanisms of polyphosphate glasses in relation to temperature and pressure. *J Non-Cryst Solids* 222:415–421
108. Gomez F, Vast P, Llewellyn P, Rouquerol F (1997) Characterization of polyphosphate glasses preparation using CRTA. *J Therm Anal* 49(3):1171–1178
109. Badens E, Llewellyn P, Fulconis JM, Jourdan C, Veesler S, Boistelle R, Rouquerol F (1998) Study of gypsum dehydration by controlled transformation rate thermal analysis (CRTA). *J Solid State Chem* 139(1):37–44
110. Gomez F, Vast P, Baebieux F, Llewellyn P, Rouquerol F (1998) Controlled transformation rate thermal analysis: an inverse method allowing the characterisation of the thermal behaviour of polyphosphate glasses. *High Temp.-High Pressures* 30(5):575–580
111. Fulconis JM, Morato F, Rouquerol F, Fourcade R, Feugier A, Rouquerol J (1999) CRTA study of the reduction of UO_2F_2 into UO_2 by dry H_2 . *J Therm Anal Calorim* 56(3):1443–1446
112. Ichihara S, Endo A, Arai T (2000) Analysis of thermal decomposition behaviors with consecutive reactions by TG. *Thermochim Acta* 360(2):179–188
113. Fesenko EA, Barnes PA, Parkes GMB, Dawson EA, Tiernan MJ (2002) Catalyst characterisation and preparation using sample controlled thermal techniques—high resolution studies and the determination of the energetics of surface and bulk processes. *Top Catal* 19(3/4):283–301

114. Fesenko EA, Barnes PA, Parkes GMB (2003) SCTA and catalysis. In: Sørensen OT, Rouquerol J (eds) *Sample controlled thermal analysis: origin, goals, multiple forms, applications and future*. Kluwer, Dordrecht, pp 174–225
115. Tiernan MJ, Barnes PA, Parkes GMB (1999) New approach to the investigation of mechanisms and apparent activation energies for the reduction of metal oxides using constant reaction rate temperature-programmed reduction. *J Phys Chem B* 103(2):338–345
116. Ogasawara H, Koga N (2014) Kinetic modeling for thermal dehydration of ferrous oxalate dihydrate polymorphs: a combined model for induction period-surface reaction-phase boundary reaction. *J Phys Chem A* 118(13):2401–2412
117. Galwey AK, Hood WJ (1979) Thermal decomposition of sodium carbonate perhydrate in the solid state. *J Phys Chem* 83(14):1810–1815
118. Koga N, Criado JM, Tanaka H (2002) A kinetic aspect of the thermal dehydration of dilithium tetraborate trihydrate. *J Therm Anal Calorim* 67(1):153–161
119. Criado JM (1980) Determination of the mechanism of thermal decomposition reactions of solids by using the cyclic and constant decomposition rate thermal analysis method. In: Wiedemann HG (ed) *Thermal analysis, Proceedings of the 6th international conference on thermal analysis*, Bayreuth, 1980. Birkhauser Verlag, Basel, pp 145–148
120. Dion P, Alcover JF, Bergaya F, Ortega A, Llewellyn PL, Rouquerol F (1998) Kinetic study by controlled-transformation rate thermal analysis of the dehydroxylation of kaolinite. *Clay Miner* 33(2):269–276
121. Tiernan MJ, Barnes PA, Parkes GMB (1999) Use of solid insertion probe mass spectrometry and constant rate thermal analysis in the study of materials: determination of apparent activation energies and mechanisms of solid-state decomposition reactions. *J Phys Chem B* 103(33):6944–6949
122. Parkes GM, Barnes PA, Charsley EL (1999) New concepts in sample controlled thermal analysis: resolution in the time and temperature domains. *Anal Chem* 71(13):2482–2487
123. Barnes PA, Tiernan MJ, Parkes GMB (1999) Sample controlled thermal analysis: temperature programmed reduction of bulk and supported copper oxide. *J Therm Anal Calorim* 56(2):733–737
124. Fesenko EA, Barnes PA, Parkes GMB, Brown DR, Naderi M (2001) A new approach to the study of the reactivity of solid-acid catalysts: the application of constant rate thermal analysis to the desorption and surface reaction of isopropylamine from NaY and HY Zeolites. *J Phys Chem B* 105(26):6178–6185
125. Tiernan MJ, Fesenko EA, Barnes PA, Parkes GMB, Ronane M (2001) The application of CRTA and linear heating thermoanalytical techniques to the study of supported cobalt oxide methane combustion catalysts. *Thermochim Acta* 379(1–2):163–175
126. Arai T, Fujii N (1997) Controlled-rate thermal analysis kinetic study in thermal dehydration of calcium sulfate dihydrate. *J Anal Appl Pyrol* 39(2):129–143
127. Cai XE, Shen H, Zhang CH, Wang YX, Kong Z (2000) Application of constant reaction rate TG to the determination of kinetic parameters by Hi-Res TG. *J Therm Anal Calorim* 60(2):623–628
128. Ortega A (1997) CRTA or TG? *Thermochim Acta* 298(1–2):205–214
129. Rouquerol J (1989) Controlled transformation rate thermal analysis: the hidden face of thermal analysis. *Thermochim Acta* 144(2):209–224
130. Ortega A, Akhouayri S, Rouquerol F, Rouquerol J (1994) On the suitability of controlled transformation rate thermal analysis (CRTA) for kinetic studies. Part 2. Comparison with conventional TG for the thermolysis of dolomite with different particle sizes. *Thermochim Acta* 235(2):197–204
131. Reading M, Dollimore D (1994) The application of constant rate thermal analysis to the study of the thermal decomposition of copper hydroxy carbonate. *Thermochim Acta* 240:117–127
132. Criado JM, Pérez-Maqueda LA (2005) Sample controlled thermal analysis and kinetics. *J Therm Anal Calorim* 80(1):27–33

133. Nahdi K, Rouquerol F, Trabelsi Ayadi M (2009) $\text{Mg}(\text{OH})_2$ dehydroxylation: a kinetic study by controlled rate thermal analysis (CRTA). *Solid State Sci* 11(5):1028–1034
134. Gotor FJ, Macias M, Ortega A, Criado JM (2000) Comparative study of the kinetics of the thermal decomposition of synthetic and natural siderite samples. *Phys Chem Miner* 27 (7):495–503
135. Sánchez-Jiménez PE, Criado JM, Pérez-Maqueda LA (2008) Kissinger kinetic analysis of data obtained under different heating schedules. *J Therm Anal Calorim* 94(2):427–432
136. Valverde JM, Sánchez-Jiménez PE, Perejon A, Pérez-Maqueda LA (2013) Constant rate thermal analysis for enhancing the long-term CO_2 capture of CaO at Ca-looping conditions. *Appl Energy* 108:108–120
137. Valverde JM, Sánchez-Jiménez PE, Perejon A, Pérez-Maqueda LA (2013) Role of looping-calcination conditions on self-reactivation of thermally pretreated CO_2 sorbents based on CaO. *Energy Fuels* 27(6):3373–3384
138. Koga N (2005) A comparative study of the effects of decomposition rate control and mechanical grinding on the thermal decomposition of aluminum hydroxide. *J Therm Anal Calorim* 81(3):595–601
139. Kimura T, Koga N (2011) Thermal dehydration of monohydrocalcite: overall kinetics and physico-geometrical mechanisms. *J Phys Chem A* 115(38):10491–10501
140. Koga N, Suzuki Y, Tatsuoka T (2012) Thermal dehydration of magnesium acetate tetrahydrate: formation and in situ crystallization of anhydrous glass. *J Phys Chem B* 116 (49):14477–14486
141. Koga N, Yamada S, Kimura T (2013) Thermal decomposition of silver carbonate: phenomenology and physico-geometrical kinetics. *J Phys Chem C* 117(1):326–336
142. Kitabayashi S, Koga N (2014) Physico-geometrical mechanism and overall kinetics of thermally induced oxidative decomposition of Tin(II) oxalate in air: formation process of microstructural Tin(IV) Oxide. *J Phys Chem C* 118(31):17847–17861
143. Wada T, Nakano M, Koga N (2015) Multistep kinetic behavior of the thermal decomposition of granular sodium percarbonate: hindrance effect of the outer surface layer. *J Phys Chem A* 119(38):9749–9760
144. Stacey MH, Shanon MD (1985) The decomposition of Cu-Zn hydroxi-carbonate solid solutions. *Mater Sci Monogr* 28:713–718
145. Sánchez-Jiménez PE, Pérez-Maqueda LA, Perejón A, Pascual-Cosp J, Benítez-Guerrero M, Criado JM (2011) An improved model for the kinetic description of the thermal degradation of cellulose. *Cellulose* 18(6):1487–1498
146. Sánchez-Jiménez PE, Pérez-Maqueda LA, Perejón A, Criado JM (2009) Combined kinetic analysis of thermal degradation of polymeric materials under any thermal pathway. *Polym Degrad Stab* 94(11):2079–2085
147. Sánchez-Jiménez PE, Pérez-Maqueda LA, Perejón A, Criado JM (2011) Constant rate thermal analysis for thermal stability studies of polymers. *Polym Degrad Stab* 96(5):974–981
148. Sánchez-Jiménez PE, Perejón A, Criado JM, Diánez MJ, Pérez-Maqueda LA (2010) Kinetic model for thermal dehydrochlorination of poly(vinyl chloride). *Polymer* 51(17):3998–4007
149. Sánchez-Jiménez PE, Pérez-Maqueda LA, Perejón A, Criado JM (2010) Generalized kinetic master plots for the thermal degradation of polymers following a random scission mechanism. *J Phys Chem A* 114(30):7868–7876
150. Arai T, Ichihara S, Nakagawa H, Fujii N (1998) A kinetic study of the thermal decomposition of polyesters by controlled-rate thermogravimetry. *Thermochim Acta* 319 (1–2):139–149
151. Sánchez-Jiménez PE, Pérez-Maqueda LA, Perejón A, Criado JM (2013) Generalized master plots as a straightforward approach for determining the kinetic model: the case of cellulose pyrolysis. *Thermochim Acta* 552:54–59
152. Sánchez-Jiménez PE, Pérez-Maqueda LA, Perejón A, Criado JM (2012) Nanoclay nucleation effect in the thermal stabilization of a polymer nanocomposite: a kinetic mechanism change. *J Phys Chem C* 116(21):11797–11807

153. Perejón A, Sánchez-Jiménez PE, Gil-González E, Pérez-Maqueda LA, Criado JM (2013) Pyrolysis kinetics of ethylene-propylene (EPM) and ethylene-propylene-diene (EPDM). *Polym Degrad Stab* 98(9):1571–1577
154. Sánchez-Jiménez PE, Pérez-Maqueda LA, Perejón A, Criado JM (2013) Limitations of model-fitting methods for kinetic analysis: Polystyrene thermal degradation. *Resour Conserv Recycl* 74:75–81
155. Miranda R, Yang J, Roy C, Vasile C (1999) Vacuum pyrolysis of PVC I. Kinetic study. *Polym Degrad Stab* 64(1):127–144
156. Miranda R, Yang J, Roy C, Vasile C (2001) Vacuum pyrolysis of commingled plastics containing PVC I. Kinetic study. *Polym Degrad Stab* 72(3):469–491
157. Kim S (2001) Pyrolysis kinetics of waste PVC pipe. *Waste Manag* 21(7):609–616
158. Jiménez A, Berenguer V, López J, Sánchez A (1993) Thermal degradation study of poly (vinyl chloride): kinetic analysis of thermogravimetric data. *J Appl Polym Sci* 50(9):1565–1573
159. Wu C-H, Chang C-Y, Hor J-L, Shih S-M, Chen L-W, Chang F-W (1994) Two-stage pyrolysis model of PVC. *Can J Chem Eng* 72(4):644–650
160. Slapak MJP, van Kasteren JMN, Drinkenburg AAH (2000) Determination of the pyrolytic degradation kinetics of virgin-PVC and PVC-waste by analytical and computational methods. *Comput Theor Polym Sci* 10(6):481–489
161. Rouquerol J (1973) Critical examination of several problems typically found in the kinetic study of thermal decomposition under vacuum. *J Therm Anal* 5(2–3):203–216
162. Rouquerol J, Ganteaume M (1977) Thermolysis under vacuum: essential influence of the residual pressure on thermoanalytical curves and the reaction products. *J Therm Anal* 11 (2):201–210
163. Rouquerol J, Rouquerol F, Ganteaume M (1975) Thermal decomposition of gibbsite under low pressures I. Formation of the boehmitic phase. *J Catal* 36(1):99–110
164. Stacey MH (1985) Applications of thermal methods in catalysis. *Anal Proc* 22(8):242–243
165. Stacey MH (1987) Kinetics of decomposition of gibbsite and boehmite and the characterization of the porous products. *Langmuir* 3(5):681–686
166. Barnes PA, Parkes GMB (1995) A new approach to catalyst preparation using rate controlled temperature programme techniques. *Stud Surf Sci Catal* 91:859–868
167. Koga N, Yamada S (2004) Controlled rate thermal decomposition of synthetic bayerite under vacuum. *Solid State Ionics* 172(1–4):253–256
168. Pérez-Maqueda LA, Criado JM, Real C, Subrt J, Bohacek J (1999) The use of constant rate thermal analysis (CRTA) for controlling the texture of hematite obtained from the thermal decomposition of goethite. *J Mater Chem* 9(8):1839–1845
169. Pérez-Maqueda LA, Criado JM, Subrt J, Real C (1999) Synthesis of acicular hematite catalysts with tailored porosity. *Catal Lett* 60(3):151–156
170. Chopra GS, Real C, Alcalá MD, Pérez-Maqueda LA, Subrt J, Criado JM (1999) Factors influencing the texture and stability of maghemite obtained from the thermal decomposition of lepidocrocite. *Chem Mater* 11(4):1128–1137
171. Salles F, Douillard JM, Denoyel R, Bildstein O, Jullien M, Beurroies I, Van Damme H (2009) Hydration sequence of swelling clays: evolutions of specific surface area and hydration energy. *J Colloid Interface Sci* 333(2):510–522
172. Belgacem K, Llewellyn P, Nahdi K, Trabelsi-Ayadi M (2008) Thermal behaviour study of the talc. *Optoelectron Adv Mat* 2(6):332–336
173. Rockmann R, Kalies G (2007) Characterization and adsorptive application of ordered mesoporous silicas. *Appl Surf Sci* 253(13):5666–5670
174. Llewellyn P, Rouquerol J (2003) SCTA and adsorbents. *J Therm Anal Calorim* 72(3):1099–1101
175. Sicard L, Llewellyn PL, Patarin J, Kolenda F (2001) Investigation of the mechanism of the surfactant removal from a mesoporous alumina prepared in the presence of sodium dodecylsulfate. *Microporous Mesoporous Mater* 44–45:195–201

176. Dufau N, Luciani L, Rouquerol F, Llewellyn P (2001) Use of sample controlled thermal analysis to liberate the micropores of aluminophosphate AlPO_4 II: evidence of template evaporation. *J Mater Chem* 11(4):1300–1304
177. Chevrot V, Llewellyn PL, Rouquerol F, Godlewski J, Rouquerol J (2000) Low temperature constant rate thermodesorption as a tool to characterise porous solids. *Thermochim Acta* 360 (1):77–83
178. Llewellyn P, Rouquerol F, Rouquerol J (2003) SCTA and Adsorbents. In: Sørensen OT, Rouquerol J (eds) *Sample controlled thermal analysis: origin, goals, multiple forms, applications and future*. Kluwer, Dordrecht, pp 135–173
179. Pérez-Maqueda LA, Sánchez-Jiménez PE, Criado JM (2007) Sample controlled temperature (SCT): a new method for the synthesis and characterization of catalysts. *Curr Top Catal* 6:1–17
180. Criado JM, Gotor FJ, Real C, Jimenez F, Ramos S, Delcerro J (1991) Application of the constant rate thermal-analysis technique to the microstructure control of BaTiO_3 yielded from coprecipitated oxalate. *Ferroelectrics* 115(1–3):43–48
181. Criado JM, Dianez MJ, Gotor F, Real C, Mundi M, Ramos S, Delcerro J (1992) Correlation between synthesis conditions, coherently diffracting domain size and cubic phase stabilization in barium-titanate. *Ferroelectrics Lett* 14(3–4):79–84
182. Gotor FJ, Real C, Dianez MJ, Criado JM (1996) Relationships between the texture and structure of BaTiO_3 and its tetragonal \rightarrow cubic transition enthalpy. *J Solid State Chem* 123 (2):301–305
183. Gotor FJ, Pérez-Maqueda LA, Criado JM (2003) Synthesis of BaTiO_3 by applying the sample controlled reaction temperature (SCRT) method to the thermal decomposition of barium titanyl oxalate. *J Eur Ceram Soc* 23(3):505–513
184. Pérez-Maqueda LA, Diánez MJ, Gotor FJ, Sayagués MJ, Real C, Criado JM (2003) Synthesis of needle-like BaTiO_3 particles from the thermal decomposition of a citrate precursor under sample controlled reaction temperature conditions. *J Mater Chem* 13 (9):2234–2241
185. Alcalá MD, Real C, Criado JM (1992) Application of constant rate thermal analysis (CRTA) to the synthesis of silicon nitride by carbothermal reduction of silica. *J Therm Anal* 38 (3):313–319
186. Alcalá MD, Criado JM, Real C (2002) Preparation of Si_3N_4 from carbothermal reduction of SiO employing the CRTA method. *Mater Sci Forum* 383:25–30
187. Alcalá MD, Criado JM, Real C (2002) Sample controlled reaction temperature (SCRT): controlling the phase composition of silicon nitride obtained by carbothermal reduction. *Adv Eng Mater* 4(7):478–482
188. Real C, Alcalá MD, Criado JM (1997) Synthesis of silicon carbide whiskers from carbothermal reduction of silica gel by means of the constant rate thermal analysis (CRTA) method. *Solid State Ionics* 95(1–2):29–32
189. Ortega A, Roldan MA, Real C (2006) Carbothermal synthesis of vanadium nitride: kinetics and mechanism. *Int J Chem Kinet* 38(6):369–375
190. Ortega A, Roldan MA, Real C (2005) Carbothermal synthesis of titanium nitride (TiN): kinetics and mechanism. *Int J Chem Kinet* 37(9):566–571
191. Real C, Alcalá MD, Criado JM (2004) Synthesis of silicon nitride from carbothermal reduction of rice husks by the constant rate thermal analysis (CRTA) method. *J Am Ceram Soc* 87(1):75–78
192. Alcalá MD, Criado JM, Real C (2001) Influence of the experimental conditions and the grinding of the starting materials on the structure of silicon nitride synthesised by carbothermal reduction. *Solid State Ionics* 141–142:657–661
193. Schaf O, Weibel A, Llewellyn PL, Knauth P, Kaabbuathong N, Vona MLD, Licoccia S, Traversa E (2004) Preparation and electrical properties of dense ceramics with NASICON composition sintered at reduced temperatures. *J Electroceram* 13(1–3):817–823
194. Dwivedi A, Speyer RF (1994) Rate-controlled organic burnout of multilayer green ceramics. *Thermochim Acta* 247(2):431–438

195. Nishimoto MY, Speyer RF, Hackenberger WS (2001) Thermal processing of multilayer PLZT actuators. *J Mater Sci* 36(9):2271–2276
196. Feylessoufi A, Crespin M, Dion P, Bergaya F, Van Damme H, Richard P (1997) Controlled rate thermal treatment of reactive powder concretes. *Adv Cem Based Mater* 6(1):21–27
197. Grillet Y, Cases JM, Francois M, Rouquerol J, Poirier JE (1988) Modification of the porous structure and surface area of sepiolite under vacuum thermal treatment. *Clays Clay Miner* 36(3):233–242
198. Bordère S, Floreancing A, Rouquerol F, Rouquerol J (1993) Obtaining a divided uranium oxide from the thermolysis of $\text{UO}_2(\text{NO}_3)_2 \cdot 6\text{H}_2\text{O}$: outstanding role of the residual pressure. *Solid State Ionics* 63–65:229–235
199. Llewellyn PL, Chevrot V, Ragai J, Cerclier O, Estienne J, Rouquerol F (1997) Preparation of reactive nickel oxide by the controlled thermolysis of hexahydrated nickel nitrate. *Solid State Ionics* 101:1293–1298
200. Arii T, Taguchi T, Kishi A, Ogawa M, Sawada Y (2002) Thermal decomposition of cerium (III) acetate studied with sample-controlled thermogravimetric–mass spectrometry (SCTG—MS). *J Eur Ceram Soc* 22(13):2283–2289
201. Nahdi K, Férid M, Ayadi MT (2009) Thermal dehydration of $\text{CeP}_3\text{O}_9 \cdot 3\text{H}_2\text{O}$ by controlled rate thermal analysis. *J Therm Anal Calorim* 96(2):455–461
202. Chehimi-Moumen F, Llewellyn P, Rouquerol F, Vacquier G, Hassen-Chehimi DB, Ferid M, Trabelsi-Ayadi M (2005) Constant transformation rate thermal analysis of $\text{HGdP}_2\text{O}_7 \cdot 3\text{H}_2\text{O}$. *J Therm Anal Calorim* 82(3):783–789

Thermal Physics and Thermal Analysis
From Macro to Micro, Highlighting Thermodynamics,
Kinetics and Nanomaterials

Šesták, J.; Hubík, P.; Mares, J. (Eds.)

2017, XXVII, 567 p. 179 illus., 83 illus. in color.,

Hardcover

ISBN: 978-3-319-45897-7